



## Emergent speciation by multiple Dobzhansky-Muller incompatibilities

Tiago Paixão, Kevin E. Bassler and Ricardo B. R. Azevedo

bioRxiv first posted online August 20, 2014

Access the most recent version at doi: <http://dx.doi.org/10.1101/008268>

---

**Creative  
Commons  
License**

The copyright holder for this preprint is the author/funder. It is made available under a [CC-BY 4.0 International license](#).

# Emergent speciation by multiple Dobzhansky–Muller incompatibilities

Tiago Paixão<sup>1,2</sup> Kevin E. Bassler<sup>3,4,5</sup> Ricardo B. R. Azevedo<sup>1,6</sup>

## Abstract

The Dobzhansky–Muller model posits that incompatibilities between alleles at different loci cause speciation. However, it is known that if the alleles involved in a Dobzhansky–Muller incompatibility (DMI) between two loci are neutral, the resulting reproductive isolation cannot be maintained in the presence of either mutation or gene flow. Here we propose that speciation can emerge through the collective effects of multiple neutral DMIs that cannot, individually, cause speciation—a mechanism we call emergent speciation. We investigate emergent speciation using a haploid neutral network model with recombination. We find that certain combinations of multiple neutral DMIs can lead to speciation. Complex DMIs and high recombination rate between the DMI loci facilitate emergent speciation. These conditions are likely to occur in nature. We conclude that the interaction between DMIs may be a root cause of the origin of species.

## Introduction

Unravelling the ways in which reproductive barriers between populations arise and are maintained remains a central challenge of evolutionary biology. The Dobzhansky–Muller model posits that speciation is driven by intrinsic postzygotic reproductive isolation caused by incompatibilities between alleles at different loci (Dobzhansky, 1937; Muller, 1942; Orr, 1995). The kinds of strong negative epistatic interactions envisioned by this model are common between amino acid substitutions within proteins (Kondrashov et al., 2002; Kulathinal et al., 2004). Furthermore, Dobzhansky–Muller incompatibilities (hereafter DMIs) have been shown to cause inviability or sterility in hybrids between closely related species, although the extent to which any particular DMI has actually contributed to speciation remains an open question (Presgraves, 2010a,b; Maheshwari and Barbash, 2011; Seehausen et al., 2014).

In Figure 1A, we illustrate a simple version of the evolutionary scenario originally proposed by Dobzhansky (1937) with an incompatibility between neutral alleles at two loci (A and B) in a

<sup>1</sup>Department of Biology and Biochemistry, University of Houston, Houston, TX 77204-5001.

<sup>2</sup>The Institute of Science and Technology Austria, Am Campus 1, Klosterneuburg 3400, Austria.

<sup>3</sup>Department of Physics, University of Houston, Houston, TX 77204-5005.

<sup>4</sup>Texas Center for Superconductivity, University of Houston, Houston, TX 77204-5002.

<sup>5</sup>Max Planck Institute for the Physics of Complex Systems, Nöthnitzer Str. 38, Dresden D-01187, Germany.

<sup>6</sup>For correspondence: razevedo@uh.edu

haploid. We refer to this interaction as a *neutral DMI*. An ancestral population is fixed for the *ab* genotype. This population splits into two geographically isolated (allopatric) populations. One population fixes the neutral allele *A* at the A locus, whereas the other fixes the neutral allele *B* at the B locus. The derived alleles are incompatible: individuals carrying one of the derived alleles are fit but individuals carrying both of them are not. Upon secondary contact between the populations, this neutral DMI creates postzygotic isolation between the two populations: if *r* is the recombination rate between the loci, then *r*/2 of haploid F<sub>1</sub> hybrids between individuals from the two populations are unfit (inviable or sterile).

The neutral DMI described in the previous paragraph is unlikely to be an effective mechanism of speciation because it assumes that the populations diverge in perfect allopatry, and that the derived alleles go to fixation before secondary contact takes place. However, either mutation or gene flow can disrupt this process (Barton and Bengtsson, 1986; Bank et al., 2012) (Figures 1B and 1C): they lead to the production of individuals with the ancestral genotype (*ab*) and these individuals have an advantage because they are completely compatible with individuals carrying derived alleles (*Ab* and *aB*).

It is known that the reproductive barriers created by neutral DMIs can be strengthened in at least two ways. First, if selection favors the derived alleles—that is, if the DMI is *not* neutral (Gavrilets, 1997; Agrawal et al., 2011; Bank et al., 2012). This could happen if the derived alleles are involved in adaptation to different environments, a scenario known as ecological speciation (Schluter, 2009; Agrawal et al., 2011). Second, if the two populations are prezygotically isolated. For example, the low fitness of hybrids can select against hybridization and cause the evolution of assortative mating between individuals carrying the same derived allele—a mechanism known as reinforcement (Dobzhansky, 1937; Felsenstein, 1981; Liou and Price, 1994; Servedio and Kirkpatrick, 1997).

Here we consider a new mechanism we call *emergent speciation*—that speciation emerges through the collective effects of multiple neutral DMIs that cannot, individually, cause speciation. Low fitness in hybrids between closely related species is often caused by multiple DMIs (Presgraves, 2003; Payseur and Hoekstra, 2005; Masly and Presgraves, 2007; Matute et al., 2010; Moyle and Nakazato, 2010; Schumer et al., 2014). However, it does not follow that any of these DMIs actually caused speciation: most of the DMIs may have accumulated after speciation had occurred by other means.

The majority of theoretical work on DMIs has relied on either population genetic models (Nei, 1976; Bengtsson and Christiansen, 1983; Wagner et al., 1994; Gavrilets and Hastings, 1996; Gavrilets, 1997; Agrawal et al., 2011; Bank et al., 2012), or models of divergence between populations (Werth and Windham, 1991; Orr, 1995; Lynch and Force, 2000b; Orr and Turelli, 2001; Welch, 2004; Fraïsse et al., 2014). Both classes of models include simplifying assumptions: the former consider only DMIs involving 2–3 loci, whereas the latter ignore polymorphism at the DMI loci. Both simplifications are problematic: reproductive isolation is often caused by multiple DMIs involving multiple loci (Presgraves, 2003; Payseur and Hoekstra, 2005; Masly and Presgraves, 2007; Matute et al., 2010; Moyle and Nakazato, 2010; Schumer et al., 2014), and many populations contain alleles

involved in DMIs segregating within them (Cutter, 2012; Corbett-Detig et al., 2013). The few studies that have attempted to overcome these simplifications have either excluded DMIs (Flaxman et al., 2014) or have not represented DMIs explicitly (Barton and Bengtsson, 1986; Gavrillets et al., 1998; Gavrillets, 1999; Barton and de Cara, 2009) and, therefore, could not capture emergent speciation. We investigate emergent speciation using a haploid neutral network model (Schuster et al., 1994; van Nimwegen et al., 1999) with recombination (Xia and Levitt, 2002; Szöllősi and Derényi, 2008), which allows us to represent DMIs involving multiple loci (Gavrillets and Gravner, 1997; Gavrillets, 2004), and to take into account genetic variation at those loci (Cutter, 2012; Corbett-Detig et al., 2013).

A neutral network (Schuster et al., 1994; van Nimwegen et al., 1999) is a network of fit genotypes connected by mutational accessibility. Two genotypes are mutationally accessible if one genotype can be obtained from the other through a single mutation. For example, Figure 1A shows a neutral network where  $aB$  is connected to  $ab$  but not to  $Ab$ . All genotypes in the network are fit and have equal fitness. All genotypes outside the network are unfit but some may be mutationally accessible from genotypes in the network. For example, in the neutral network shown in Figure 1A,  $AB$  is unfit, and it is accessible from both  $aB$  and  $Ab$ , but not  $ab$ .

Neutral networks define “holey” adaptive landscapes with “ridges” of fit genotypes connecting distant genotypes (Gavrillets and Gravner, 1997; Gavrillets, 2004). They extend the neutral DMI model to multiple loci (Gavrillets and Gravner, 1997; Gavrillets, 2004); a neutral network of  $K$  genotypes with  $L$  loci, each with  $\alpha$  alleles can be constructed by taking the entire space of  $\alpha^L$  genotypes and “removing” the  $\alpha^L - K$  genotypes that carry incompatible combinations of alleles (e.g., the  $A$  and  $B$  alleles in the neutral network in Figure 1A). A single DMI of order  $\omega$  (i.e., one involving alleles at  $\omega$  loci) implies the removal of  $\alpha^{L-\omega}$  genotypes ( $2 \leq \omega \leq L$ ). Additional DMIs imply the removal of other genotypes, although the corresponding sets of genotypes to remove may overlap with each other. DMIs of order  $\omega = 2$  are designated *simple*, whereas those of order  $\omega > 2$  are designated *complex* (Cabot et al., 1994; Orr, 1995; Fraïsse et al., 2014). DMIs of order up to  $\omega = 5$  have been discovered in introgression studies (Fraïsse et al., 2014). The alleles of genotypes in the neutral network can be, for example, nucleotides, amino acids, insertions/deletions, or presence/absence of functional genes. Therefore, a neutral network can also be used to represent DMI-like scenarios such as the degeneration of duplicate genes (Werth and Windham, 1991; Lynch and Force, 2000b; Nei and Nozawa, 2011).

We show that neutral networks defined by multiple simple and/or complex neutral DMIs can lead to the establishment of stable reproductive barriers between populations. Although the neutral network model includes its own simplifying assumptions, it captures the essence of the phenomenon of emergent speciation in the absence of other possible mechanisms of speciation. Thus, it allows us to identify and characterize some of the causes of emergent speciation, including the pattern of interactions between DMI loci and recombination. Furthermore, emergent speciation is a robust mechanism that we argue should operate under a broad range of conditions.

## Results

### A neutral DMI between two loci is not sufficient to cause speciation

Consider the neutral DMI illustrated in Figure 1A. Initially, two allopatric populations are fixed for the  $aB$  and  $Ab$  genotypes, respectively. The populations are maximally genetically differentiated at the two loci ( $G_{ST} = 1$ ). The degree of reproductive isolation between the two populations is  $I = r/2$ , the mean fitness of haploid  $F_1$  hybrids between individuals from the two populations (see Materials and methods for definitions of both  $G_{ST}$  and  $I$ ).

How stable is the reproductive barrier between the two populations? To address this question we begin by investigating the effect of mutation within populations. If the alleles at each locus can mutate into each other ( $A \leftrightarrow a$  and  $B \leftrightarrow b$ ) at a rate  $u$  per locus per generation, then the degree of reproductive isolation will decline exponentially according to the expression:  $I_t \approx I_0 \cdot e^{-2ut}$ , where  $t$  is time in generations, and  $I_0 = r/2$  is the initial reproductive isolation. For example, if  $u = 10^{-3}$  and  $r = 0.2$ , then genetic differentiation and reproductive isolation will be eliminated within  $\sim 4,000$  generations (Figures 1B and 1C,  $m = 0$ ). Any amount of gene flow between the two populations will further accelerate the erosion of the reproductive barrier (Figures 1B and 1C,  $m > 0$ ). For example, if just 1 individual in 2,000 migrates from one population to the other every generation ( $m = 0.0005$ ) then genetic differentiation and reproductive isolation will be eliminated within  $\sim 2,000$  generations.

The evolution of a stable reproductive barrier between two populations—that is, speciation—requires the existence of more than one stable equilibrium (Barton, 1996; Gavrilets and Hastings, 1996). A single neutral DMI between two diallelic loci is not sufficient to cause speciation because, in the presence of mutation ( $0 < u < 0.5$ ), it only contains one stable equilibrium for any level of recombination (Gavrilets, 2004), and populations will gradually evolve toward this equilibrium (Figure 1—figure supplement 1). Changes to the adaptive landscape can cause the appearance of two stable equilibria (Bank et al., 2012). For example, if the derived alleles confer an advantage (fitness:  $w_{aB} = w_{Ab} = 1$  and  $w_{ab} = 1 - s$ ), and if both  $r$  and  $s \gg u$ , the genotype network will have two stable equilibria, with  $\hat{p}_{Ab} \approx 1$  and  $\hat{p}_{aB} \approx 1$ , respectively (Figure 2). Two populations in different equilibria will show a degree of reproductive isolation of:  $I \approx r(1 + s)/2$  (Figure 2E).

### Neutral networks based on multiple DMIs can show multiple stable equilibria

We began by investigating whether neutral networks contain multiple stable equilibria. To do this we generated ensembles of 500 random neutral networks of  $K$  genotypes with  $L$  loci and  $\alpha$  alleles per locus for a range of values of  $K$ ,  $L$  and  $\alpha$ . None of the neutral networks considered could have been specified by a single DMI of any order ( $2 \leq \omega \leq L$ ). To construct a random neutral network, we generated  $K$  random genotypes with  $L$  loci and one of  $\alpha$  alleles per locus, and kept the resulting network if it was connected. We ignored disconnected networks because, although they often contain multiple stable equilibria, a population is unlikely to shift from one equilibrium to another because it requires rare multiple mutations (Gavrilets, 2004).

For each neutral network, we constructed populations with different initial genotype frequencies and allowed each population to evolve independently until it reached equilibrium. We then evaluated the stability of the resulting equilibria (see Materials and methods). No neutral networks defined on  $L = 3$  loci with  $\alpha = 2$  alleles per locus contain multiple stable equilibria. However, some neutral networks with  $L = 4$  and  $\alpha = 2$ , and with  $L = 3$  and  $\alpha = 3$  contain multiple stable equilibria (Figure 3A; Figure 3—figure supplement 1A). Populations evolving independently to different stable equilibria become genetically differentiated and partially reproductively isolated from each other (Figure 3B–C; Figure 3—figure supplement 1B–C). Thus, speciation can emerge through the collective effects of multiple neutral DMIs that cannot, individually, cause speciation.

### **Larger, sparser neutral networks are more likely to contain multiple stable equilibria**

The probability,  $P_M$ , that a random neutral network from an ensemble shows multiple stable equilibria is correlated with properties of the network.  $P_M$  increases with the size of the network,  $K$  (Figure 3A; Figure 3—figure supplement 1A). We have never found any random connected neutral network with  $K = 5$  genotypes with multiple equilibria ( $P_M \approx 0$ ), regardless of the values of  $L$  and  $\alpha$ . In contrast, networks with  $K = 9$  genotypes defined by  $L = 6$  diallelic loci, show  $P_M \approx 50\%$ .

For random neutral networks of a given size, the topology of the network also influences  $P_M$ . This is the reason why the relationship between  $P_M$  and  $K$  is non-monotonic for  $L = 4$  diallelic loci (Figure 3A): the genotype space consists of only  $2^4 = 16$  genotypes, which constrains the range of topologies that a random neutral network can take. Increasing either  $L$  or  $\alpha$  increases the size of the genotype space and, therefore, alleviates the constraint (Figure 3A; Figure 3—figure supplement 1A).

Table 1 shows that  $P_M$  is correlated with multiple network properties, including the average degree of a genotype, that is, the mean number of mutational neighbors it has in the neutral network. One complication is that different properties of neutral networks are not independent of each other (Table 1; Figure 3—figure supplement 3). Figure 3—figure supplement 2 shows two network correlates of  $P_M$  that are, in turn, uncorrelated with each other (Figure 3—figure supplement 3; Table 1): the spectral radius and the degree assortativity. The spectral radius is the leading eigenvalue of the adjacency matrix and measures the mean degree of a population at equilibrium when  $r = 0$  (van Nimwegen et al., 1999). The degree assortativity measures the extent to which nodes with a certain degree are connected with nodes with similar degree. Neutral networks with low spectral radius and negative degree assortativity—and more sparsely connected, spread out, modular networks—are more likely to show multiple stable equilibria (Table 1). However, the topology of a network is not sufficient to determine  $P_M$ : the precise pattern of linkage between loci also influences whether a particular neutral network shows multiple stable equilibria (Figure 3—figure supplement 4).

## Neutral networks based on complex DMIs are more likely to show multiple stable equilibria

A neutral network of a certain size ( $K$ ) can be specified by either a few low-order DMIs or many high-order DMIs. To investigate the extent to which DMIs of different order ( $\omega$ ) can lead to multiple stable equilibria, we have exhaustively enumerated all possible combinations of simple DMIs ( $\omega = 2$ ) on  $L = 4$  diallelic loci specifying connected neutral networks with  $K \geq 6$  genotypes. Of the 2,918 resulting neutral networks, none were found to contain multiple stable equilibria ( $P_M \approx 0$ ).

This result is surprising because random neutral networks with  $K = 6$  to 12 genotypes with  $L = 4$  diallelic loci showed  $P_M \approx 12\%$  (Figure 3A). One possibility is that simple DMIs are not sufficient to generate neutral networks with multiple stable equilibria, and that complex DMIs ( $\omega > 2$ ) are required.

To test this hypothesis, we generated additional ensembles of random neutral networks of  $K = 9$  genotypes using random combinations of DMIs of order  $\omega = 2$  to 4 between  $L = 6$  diallelic loci. We found that, although simple DMIs are capable of generating neutral networks with multiple stable equilibria,  $\sim 97\%$  of neutral networks generated by combinations of 5–14 simple DMIs have only one stable equilibrium. As expected,  $P_M$  increases with the complexity ( $\omega$ ) of the DMIs (Figure 4).

## The existence of multiple stable equilibria depends on the recombination rate

In the absence of recombination between the loci defining a neutral network, there is only one stable equilibrium (van Nimwegen et al., 1999). The genotype frequencies at equilibrium are given by the leading eigenvector of the mutation matrix  $\mathbf{M}$ , where entry  $M_{ij}$  is the mutation rate from genotype  $i$  to genotype  $j$  per generation (van Nimwegen et al., 1999). With recombination, however, multiple stable equilibria can occur (Figure 3A).

To quantitatively investigate the relationship between the existence of multiple stable equilibria and the recombination rate between fitness loci ( $r$ ) in a concrete example we considered the neutral network shown in Figure 5A. This was one of the random neutral networks in the  $K = 6$ ,  $L = 3$  and  $\alpha = 3$  ensemble summarized in Figure 3—figure supplement 1. The neutral network is defined by 10 simple DMIs:  $A_1-B_3$  (i.e.,  $A_1$  and  $B_3$  are incompatible),  $A_2-B_2$ ,  $A_2-B_3$ ,  $A_3-B_2$ ,  $A_3-B_3$ ,  $B_1-C_1$ ,  $B_1-C_3$ ,  $B_3-C_1$ ,  $B_3-C_2$ , and  $B_3-C_2$ . We examined how the number of stable equilibria in this neutral network changes with  $r$  while keeping the mutation rate constant ( $u = 10^{-3}$ ). When the recombination rate is low ( $0 \leq r < 0.0019$ ) the neutral network contains only one stable equilibrium regardless of initial conditions (Figure 5B). The equilibrium is symmetric in that the frequency of the  $A_1B_2$  haplotype (red) is the same as that of the  $B_1C_2$  haplotype (blue). Above a critical recombination rate ( $0.0019 \leq r \leq 0.5$ ) there are two stable equilibria and one unstable equilibrium. Populations evolve to the different equilibria depending on initial conditions (Figure 5C). The stable equilibria are asymmetric with an excess of genotypes containing either the  $A_1B_2$  (red) or  $B_1C_2$  (blue) haplotype, respectively (note, however, that these equilibria are symmetric with each other). The unstable equilibrium is symmetric, with equal frequencies of the  $A_1B_2$  and  $B_1C_2$  haplotypes. The critical point at which the equilibria bifurcate is approximately invariant with the  $r/u$  ratio

(Figure 5—figure supplement 1).

## **The reproductive barriers generated by multiple neutral DMIs can persist in the presence of gene flow**

If two allopatric populations evolve independently to the different stable equilibria of the neutral network in Figure 5A, they will become genetically differentiated and reproductively isolated to an extent that also depends on  $r$  (Figure 5D–E).

The reproductive barrier created by the neutral network in Figure 5A can persist in the presence of gene flow (Figures 5D–E, red). Introducing gene flow weakens the degree of genetic differentiation and of reproductive isolation at equilibrium, and increases the critical value of  $r$  required for the persistence of a reproductive barrier (Figures 5D–E, red). However, the maximum migration rate between two populations that allows the reproductive barrier to persist is lower than the mutation rate ( $m \approx 0.00047$ , for  $r = 0.5$ ; Figure 5—figure supplement 2, blue). Stable differentiation can occur in a stepping-stone model (Kimura, 1952) with higher local migration rates (Figure 6D), but the resulting reproductive barrier does not slow down the spread of a neutral allele at an unlinked locus appreciably (Barton and Bengtsson, 1986) (Table 2).

Larger neutral networks, involving complex incompatibilities between greater numbers of loci, can generate stronger reproductive barriers, capable of withstanding substantial gene flow. The neutral network shown in Figure 7A contains three stable equilibria. This was one of the random neutral networks in the  $K = 11$  and  $L = 5$  ensemble summarized in Figure 3. The neutral network is defined by 9 DMIs, 7 of which are complex:  $A-e$  (i.e.,  $A$  and  $e$  are incompatible),  $B-e$ ,  $A-b-D$ ,  $a-B-d$ ,  $A-C-D$ ,  $B-c-d$ ,  $b-C-D$ ,  $C-D-e$ , and  $a-c-d-E$ . Populations at the equilibria at opposite ends of the network can show high levels of genetic differentiation and reproductive isolation (Figures 7D and 7E). If the fitness loci are unlinked ( $r = 0.5$ ), then 50% of  $F_1$  hybrids between two populations at equilibrium are unfit. The maximum migration rate between two populations that allows the reproductive barrier to persist is almost two orders of magnitude higher than the mutation rate ( $m \approx 0.0943$ , for  $r = 0.5$ ; Figure 5—figure supplement 2, red). In a stepping-stone model, this neutral network can slow down the spread of a neutral allele at an unlinked locus to a greater extent than a single DMI with selection for the derived alleles (Figures 6C and 6E; Table 2). Thus, emergent speciation could, in principle, be an effective mechanism of either allopatric or parapatric speciation.

## **The probability of a stochastic shift from one stable equilibrium to the other decreases with the recombination rate**

In the neutral network model speciation requires that a population undergo a stochastic shift from one stable equilibrium to another. One mechanism by which this could happen is the “founder effect” (Templeton, 1980; Carson and Templeton, 1984). In this scenario, a new allopatric population is founded by a few individuals from a larger source population. The new population then expands rapidly. The stochastic shift occurs during the short period of time while the population is small.

We investigated the probability of a stochastic shift in the neutral network shown in Figure 5A (see Materials and methods). We found that the probability that a founder event causes a stochastic shift ( $P_S$ ) can be high when  $r$  is low, and declines as  $r$  increases (Figure 5F). A similar relationship between  $P_S$  and  $r$  was observed for the neutral network in Figure 7A and for a single DMI with selection for the derived alleles (Figure 7F and 2F). In general,  $P_S$  declined as the reproductive barrier became stronger (Table 2).

## Discussion

Our main result is that, when it comes to multiple neutral DMIs, the whole can be greater than the sum of its parts. Although a single neutral DMI cannot lead to the evolution of stable reproductive isolation, the collective effects of certain combinations of multiple neutral DMIs can lead to the evolution of strong barriers to gene flow between populations—a mechanism we call *emergent speciation*.

Emergent speciation depends on two factors: the pattern of interactions between DMI loci and recombination. DMIs of higher order ( $\omega$ ), and involving greater numbers of loci ( $L$ ), tend to promote emergent speciation (Figures 3 and 4). This relationship is mediated by several properties of the neutral networks specified by the DMIs: larger ( $K$ ), more sparsely connected, spread out, modular neutral networks tend to facilitate emergent speciation (Figure 3; Figure 3—figure supplement 2; Table 1). Note that our results are conservative because we considered only connected networks. Real neutral networks might, in fact, be disconnected (Jiménez et al., 2013) which would be expected to further facilitate emergent speciation.

Increasing the recombination rate between DMI loci promotes emergent speciation in at least three ways. First, it causes the appearance of multiple equilibria (Figures 5B–C and 7B–C). Recombination had been shown to generate multistability in other evolutionary models (Bürger, 1989; Bergman and Feldman, 1992; Boerlijst et al., 1996; Higgs, 1998; Wright et al., 2003; Jacobi and Nordahl, 2006; Park and Krug, 2011), although earlier studies of the evolutionary consequences of recombination in neutral networks did not detect multiple equilibria (Xia and Levitt, 2002; Szöllősi and Derényi, 2008). Second, it increases genetic differentiation between populations at the different equilibria (Figures 5D and 7D). This pattern is consistent with the observation that increasing  $r$  reduces variation within a population at equilibrium in a neutral network (Xia and Levitt, 2002; Szöllősi and Derényi, 2008; Paixão and Azevedo, 2010). Third, it increases the degree of reproductive isolation between populations at different equilibria (Figures 5E and 7E). This is because, in our model, recombination is required to produce hybrids and consequently is the predominant source of selection. High  $r$  between fitness loci has been shown to promote speciation in other models (Felsenstein, 1981; Bank et al., 2012).

The precise pattern of recombination—that is, linkage—between loci can also determine the existence of multiple equilibria (Figure 3—figure supplement 4). This result indicates that certain chromosomal rearrangements may facilitate emergent speciation. Note that this mechanism of chro-

mosomal speciation does not assume that different chromosomal rearrangements are polymorphic within populations and therefore is not based on suppression of recombination (Faria and Navarro, 2010).

How likely is emergent speciation to occur in nature? One recent study (Corbett-Detig et al., 2013) found evidence that multiple simple DMIs involving loci with high  $r$  are currently segregating within natural populations of *Drosophila melanogaster*. Corbett-Detig and colleagues surveyed a large panel of recombinant inbred lines (RILs) (Corbett-Detig et al., 2013). They found 22 incompatible pairs of alleles at unlinked loci in the RILs; of the 44 alleles, 27 were shared by two or more RILs, indicating that multiple DMIs are polymorphic within natural populations (Corbett-Detig et al., 2013). They also found evidence for multiple DMIs in RIL panels in *Arabidopsis* and maize (Corbett-Detig et al., 2013). Corbett-Detig and colleagues did not attempt to identify DMIs among linked loci or complex DMIs and therefore are likely to have underestimated the actual number and complexity of DMIs in the RILs. These observations suggest that the conditions for emergent speciation by multiple DMIs may indeed occur in nature, although the resulting neutral networks remain to be discovered.

There is strong evidence that DMIs contribute to reproductive isolation between closely related species, but it is difficult to determine the extent to which these DMIs actually caused speciation or are simply a by-product of divergence after speciation had occurred by other means (Presgraves, 2010a,b; Maheshwari and Barbash, 2011; Seehausen et al., 2014). One prediction of the emergent speciation hypothesis is that, if multiple DMIs contribute to speciation then DMIs fixed between species should have higher order ( $\omega$ ), on average, than DMIs segregating within species. Recent surveys have concluded that complex DMIs, as well as other forms of high-order epistasis, are widespread (Presgraves, 2010a; Weinreich et al., 2013; Fraïsse et al., 2014), but a systematic comparison between the complexity of DMIs in divergence and polymorphism remains to be carried out.

The neutral network model includes two central assumptions: neutrality within the network and complete unfitness outside it. Both assumptions are plausible in the case of speciation by reciprocal degeneration or loss of duplicate genes. Gene duplication followed by reciprocal degeneration or loss of duplicate copies in different lineages can act just like a DMI (Werth and Windham, 1991; Lynch and Force, 2000b), despite not involving an epistatic interaction (Nei and Nozawa, 2011). If the duplicates are essential genes, then genotypes carrying insufficient functional copies will be completely unfit. Gene duplications, degenerations and losses are common (Force et al., 1999; Lynch and Conery, 2000; Nei and Nozawa, 2011) and a substantial fraction of gene degenerations and losses are likely to be effectively neutral (Force et al., 1999; Lynch and Force, 2000a; Lynch and Conery, 2000). Following whole genome duplications, multiple gene degenerations or losses occur (Force et al., 1999; Lynch and Force, 2000a; Scannell et al., 2006; Nei and Nozawa, 2011), and the duplicates tend to be unlinked. Thus, we predict that emergent speciation will play a major role in speciation by reciprocal degeneration or loss of duplicate genes. This form of speciation appears to have contributed to the diversification of yeasts (Scannell et al., 2006).

The assumption of “in-network” neutrality is challenged by evidence that many DMI loci have experienced positive selection during their evolutionary history (Presgraves, 2010a,b; Maheshwari and Barbash, 2011). However, the neutral network model could still apply to some of those cases for two reasons. First, emergent speciation is robust to some variation in fitness among the genotypes in a neutral network (Figure 5—figure supplement 3). Second, neutral networks may approximate more complex scenarios where selection is weak or variable over time and/or space, or population sizes are small (Gavrilets, 2004).

The assumption that “out-of-network” genotypes are completely unfit is contradicted by the observation that many DMIs cause only partial loss of fitness (Presgraves, 2003; Corbett-Detig et al., 2013; Schumer et al., 2014). However, our results also apply to partial DMIs. As long as the disadvantage of “falling off” the neutral network is substantial, partial DMIs are still expected to lead to the evolution of stable—albeit weaker—reproductive barriers (Figure 5—figure supplement 4). We conclude that emergent speciation is a robust mechanism that should operate under a broader range of conditions violating the two central assumptions of the neutral network model.

The best studied examples of DMIs are in diploids (Presgraves, 2010b; Maheshwari and Barbash, 2011). Our model assumes haploidy, which means that it is mathematically equivalent to a diploid model where the incompatible haplotypes cause dominant incompatibilities, but where the same diploid genotypes involving cis and trans allele combinations (e.g.,  $Ab/aB$  and  $ab/AB$ ) may have different fitnesses. The latter is rare, and the former is unrealistic: DMIs in diploids tend to be recessive (Presgraves, 2003; Masly and Presgraves, 2007). Nevertheless, diploidy is likely to facilitate emergent speciation for three reasons. First, segregation in diploids has many of the same consequences as high recombination in haploids, regardless of the rate of recombination among linked loci (Otto, 2003). Second, diploids can show much stronger reproductive isolation than haploids. Strong reproductive isolation in haploids requires that a large proportion of recombinants carry incompatible combinations of alleles. This can only be achieved with large numbers of DMI loci and high recombination rate between them. In contrast, single DMIs can cause dramatic loss of fitness in  $F_1$  hybrids in diploids (Presgraves, 2010b; Maheshwari and Barbash, 2011). Third, diploidy may allow patterns of DMI interaction that increase the probability of stochastic shifts between stable equilibria (Wagner et al., 1994; Gavrilets, 2004).

Recombination does oppose emergent speciation in neutral networks in one crucial way: it reduces the probability of a stochastic shift ( $P_S$ ) between stable equilibria (Figures 5F and 7F).  $P_S$  also appears to increase with the strength of the reproductive barrier at equilibrium (Figures 5F and 7F). Similar observations have been made in other models (Figure 2F) (Wagner et al., 1994; Barton, 1996; Gavrilets, 2004), leading many to conclude that genetic drift alone cannot cause speciation (Barton, 1996; Seehausen et al., 2014). It does not follow, however, that emergent speciation is unlikely. Shifts between stable equilibria might be facilitated by transient changes in selection (Barton, 1996). Alternatively, populations could diverge in allopatry as envisaged in traditional DMI models (Dobzhansky, 1937; Muller, 1942; Orr, 1995).

Our results have broader implications for evolutionary theory. The neutral network model was originally developed in the context of RNA and protein sequence evolution (Lipman and Wilbur, 1991; Schuster et al., 1994; Huynen et al., 1996), and has played an important role in the study of the evolution of robustness and evolvability (Huynen et al., 1996; van Nimwegen et al., 1999; Ancel and Fontana, 2000; Wagner, 2008; Draghi et al., 2010). One limitation of much of this work is that it has been conducted using the asexual version of the neutral network model. Our finding that recombination promotes the appearance of multiple stable equilibria in neutral networks has clear implications for the evolution of robustness and evolvability that deserve further investigation. For example, Wagner (2011) has argued that recombination helps explore genotype space because it causes greater genotypic change than mutation. However, our results suggest that, depending on the structure of the neutral network, large sexual populations can get trapped in stable equilibria, therefore restricting their ability to explore genotype space.

We have found that multiple neutral DMIs can cause emergent speciation and that the conditions that promote emergent speciation are likely to occur in natural populations. We conclude that the interaction between DMIs may be a root cause of the origin of species. Continued efforts to detect DMIs (Payseur and Hoekstra, 2005; Masly and Presgraves, 2007; Schumer et al., 2014) and to reconstruct real neutral networks (Lee et al., 1997; Jiménez et al., 2013) will be crucial to evaluating the reality and importance of emergent speciation.

## Materials and methods

### Neutral network model

Organisms are haploid and carry  $L$  loci with effects on fitness. Each locus can have one of  $\alpha$  alleles. Out of the possible  $\alpha^L$  genotypes,  $K$  are fit, with equal fitness, and the remaining genotypes are completely unfit. The  $K$  genotypes define a neutral network, where genotypes are connected if one genotype can be obtained from the other through a single mutation (i.e., they differ at a single locus).

### Random neutral networks

Ensembles of random neutral networks were analyzed. Random neutral networks were generated by sampling  $K$  genotypes at random from the  $\alpha^L$  possible genotypes available (without replacement) and retaining the resulting network if it was connected.

### Neutral networks specified by DMIs

To investigate the effect of the order ( $\omega$ ) of a DMI, ensembles of neutral networks were generated by sampling combinations of  $d$  random DMIs with pre-specified values of  $\omega$  between alleles at  $L$  diallelic loci (see Figure 4 for more details). Following Orr (Orr, 1995), one allele at each locus was

considered to be ancestral and compatible with other ancestral alleles, and no DMIs were allowed where all the  $\omega$  incompatible alleles were ancestral.

## Network statistics

**Algebraic connectivity** Second smallest eigenvalue of the Laplacian matrix of the network (Newman, 2010). Abbreviated as AC in Figure 3—figure supplement 3. Calculated using NetworkX (Hagberg et al., 2008).

**Average degree and variance in degree** Mean and variance of the degree distribution, respectively (Newman, 2010). The degree of a genotype is the number of its fit mutational neighbors. Calculated using NetworkX (Hagberg et al., 2008).

**Average Hamming distance** Average number of loci at which pairs of genotypes carry different alleles. Genotypes connected in the neutral network are at a Hamming distance of 1.

**Average shortest path length** Average number of steps along the shortest path between pairs of genotypes (Newman, 2010). Abbreviated as PL in Figure 3—figure supplement 3. Calculated using NetworkX (Hagberg et al., 2008).

**Degree assortativity** A measure of the correlation of the degree of linked genotypes (Newman, 2010). Abbreviated as DA in Figure 3—figure supplement 3 and Table 1. Calculated using NetworkX (Hagberg et al., 2008).

**Estrada index** A centrality measure (Estrada and Rodríguez-Velázquez, 2005). Calculated using NetworkX (Hagberg et al., 2008).

**Modularity** A measure of the extent to which the network displays community structure (Newman, 2006). A community is a group of densely interconnected nodes showing relatively few connections to nodes outside the community. Abbreviated as Q in Figure 3—figure supplement 3. Calculated using igraph (Csárdi and Nepusz, 2006) based on an exhaustive search over all possible partitions of the network.

**Spectral radius** Leading eigenvalue of adjacency matrix (Newman, 2010). Measures the mean degree of a population at equilibrium in the absence of recombination (van Nimwegen et al., 1999). Abbreviated as SR in Figure 3—figure supplement 3 and Table 1. Calculated using NumPy (Oliphant, 2007).

## 430 Evolution

431 Evolution on a neutral network was modeled by considering an infinite-sized population of haploid  
 432 organisms reproducing sexually in discrete generations. The state of the population is given by  
 433 a vector of frequencies  $\vec{p} = (p_0, p_1, \dots, p_K)$ , where  $p_i$  is the frequency of genotype  $i$ . Genotypes  
 434 outside the network are ignored because they are completely inviable (van Nimwegen et al., 1999).  
 435 Individuals mate at random with respect to genotype to form a transient diploid that undergoes  
 436 meiosis to produce haploid descendants. Selection takes place during the haploid phase. Mating,  
 437 recombination, mutation and selection cause the population to evolve according to the equation:

$$\vec{p}_{t+1} = \frac{(\vec{p}_t \cdot \vec{\mathbf{R}} \cdot \vec{p}_t^T) \cdot \mathbf{M}}{\sum_{i=1}^K [(\vec{p}_t \cdot \vec{\mathbf{R}} \cdot \vec{p}_t^T) \cdot \mathbf{M}]_i}, \quad (1)$$

438 where  $\vec{p}_t$  is the state of the population at generation  $t$ ,  $\mathbf{M}$  is the mutation matrix such that entry  
 439  $M_{ij}$  is the mutation rate from genotype  $i$  to genotype  $j$  per generation, and  $\vec{\mathbf{R}} = (\mathbf{R}^0, \mathbf{R}^1, \dots, \mathbf{R}^K)$   
 440 is a vector of recombination matrices such that entry  $R_{i,j}^g$  of matrix  $\mathbf{R}^g$  is the probability that  
 441 a mating between individuals of genotypes  $i$  and  $j$  generates an individual offspring of genotype  
 442  $g$ . The diagonal elements of  $\mathbf{M}$  ( $M_{ii}$ ) represent the probability that genotype  $i$  does not mutate  
 443 (including to unfit genotypes outside the neutral network). Values of  $M_{ij}$  are set by assuming that  
 444 each locus mutates with probability  $u$  and that a genotype can only mutate simultaneously at up  
 445 to a certain number of loci. Up to  $L - 1$  crossover events can occur between two genotypes with  
 446 probability  $0 \leq r \leq 0.5$  per interval. The recombination rate  $r$  is the same for all pairs of adjacent  
 447 loci. If  $r = 0.5$ , then there is free recombination between all loci.

## 448 Equilibria

449 Given a neutral network, population genetic parameters  $u$  and  $r$ , and a set of initial genotype  
 450 frequencies  $\vec{p}_0$ , the population was allowed to evolve until the root-mean-square deviation of the  
 451 genotype frequencies in consecutive generations was  $\text{RMSD}(\vec{p}_t, \vec{p}_{t-1}) < 10^{-9}$ . The final genotype  
 452 frequencies were identified as an equilibrium  $\hat{p}$ . Multiple initial conditions were used: (i) fixed for  
 453 each of the  $K$  genotypes in turn, and (ii) 4 independent sets of random frequencies. Two equilibria  
 454 ( $\hat{p}_i$  and  $\hat{p}_j$ ) were judged identical if  $\text{RMSD}(\hat{p}_i, \hat{p}_j) < 3 \times 10^{-4}$ . Only one of a set of identical  
 455 equilibria was counted. This procedure does not guarantee the discovery of all equilibria; indeed, it  
 456 likely underestimates the number of unstable equilibria.

## 457 Stability analysis

458 For each equilibrium  $\hat{p}$ , the eigenvalues of the Jacobian matrix of  $\vec{p}_{t+1}$  ( $\lambda_1, \lambda_2, \dots, \lambda_K$ ) were calcu-  
 459 lated at  $\hat{p}$ . If  $|\lambda_i| < 1$  for every  $i$  (to within a tolerance of  $10^{-8}$ ), the equilibrium was judged to be  
 460 stable.

## Gene flow

Gene flow was modeled as symmetric migration between two populations. Migration occurs at the beginning of each generation, such that a proportion  $m$  of each population is composed of immigrants from the other population. Then random mating, recombination and mutation take place within each population, as described above.

## Stepping-stone model

A stepping-stone model (Kimura, 1952) was used to measure the rate of spread of a neutral allele across a reproductive barrier (Barton and Bengtsson, 1986). A number  $n$  of populations are arranged in a line. Every generation a proportion  $2m$  of a population emigrates to its two neighboring populations (except populations 1 and  $n$ , which have only one neighbor, so only  $m$  of each of them emigrate) (see Figure 6A). Note that, unlike the stepping stone model studied by Gavrillets (Gavrillets, 1997), our implementation allows the genotype frequencies of terminal populations (1 and  $n$ ) to vary. When  $n = 2$  this model reduces to the gene flow model described in the previous section.

## Genetic differentiation

$G_{ST} = 1 - H_S/H_T$  was used to measure the genetic differentiation between two populations at a locus, where  $H_S$  is the average gene diversity of the two populations, and  $H_T$  is the gene diversity of a population constructed by pooling the two populations (Nei, 1976). The gene diversity of a population at a locus is defined as  $H = 1 - \sum_{i=1}^{\alpha} q_i^2$ , where  $q_i$  is the frequency of allele  $i$ . Values of  $G_{ST}$  can vary between 0 (two populations with the same allele frequencies) and 1 (two populations fixed for different alleles). The overall genetic differentiation between two populations was quantified as the average  $G_{ST}$  over all loci. If all genotypes in the neutral network contain the same allele at a locus, that locus is excluded from the calculation of average  $G_{ST}$ .

## Reproductive isolation

The degree of reproductive isolation is defined as (Barton, 1996; Palmer and Feldman, 2009):  $I = 1 - \bar{w}_H/\bar{w}_S$ , where  $\bar{w}_H$  is the mean fitness of haploid  $F_1$  hybrid offspring from crosses between individuals from the two populations, and  $\bar{w}_S$  is the average of the mean fitnesses of the individual populations. The calculation of  $\bar{w}_H$  and  $\bar{w}_S$  only takes into account the contribution of recombination, and ignores mutation. Values of  $I$  can vary between 0 (the populations are undifferentiated or  $r = 0$ ) and 1 (all  $F_1$  hybrids are unfit).

## Founder effect speciation

To simulate a founder event (Templeton, 1980; Carson and Templeton, 1984), a new population is founded from a sample of  $N_0$  individuals from an infinite-sized population at one stable equilibrium. The population is then allowed to grow according to the equation  $N_t = \lambda^t N_0$ , where  $t$  is the

generation number and  $\lambda$  is the finite rate of increase. At generation  $t$ , the expected vector of genotype frequencies  $\vec{p}_t$  is calculated using equation (1) and a random sample of size  $N_t$  is drawn from a multinomial distribution with probabilities  $\vec{p}_t$ . Once the population reaches  $N_t > 10^4$  individuals, it is allowed to evolve deterministically to equilibrium. If the population evolves to a different equilibrium from that of the source population, it is counted as a shift.

For the adaptive landscape in Figure 2A, every simulation run was evolved to equilibrium. For the neutral network in Figure 5A, only simulation runs where at least one of the  $N_0$  founder individuals carried the  $A_1B_2$  haplotype were evolved to equilibrium. Similarly, for the neutral network Figure 7A, only simulation runs where at least one of the  $N_0$  founder individuals carried either the  $D$  allele or the  $abde$  haplotype were evolved to equilibrium. Thus, the estimates of the probability that a founder event causes a stochastic shift ( $P_S$ ) for the neutral networks in Figures 5A and 7A slightly underestimate the true value because mutations occurring early during the population expansion phase could cause a shift.

To estimate the probability that a founder event causes a stochastic shift ( $P_S$ ) as many tries ( $\nu$ ) as required to get  $\sigma$  successful shifts were run. The following unbiased estimator was used:

$$P_S = \frac{\sigma - 1}{\sigma + \nu - 1} \quad .$$

95% confidence intervals were calculated by parametric bootstrapping: for each estimate of  $P_S$ ,  $10^6$  random samples of  $\sigma$  values from the negative binomial distribution with probability of success  $P_S$  were generated and  $P_S$  was recalculated; the confidence intervals were estimated as the 2.5% and 97.5% quantiles of the distribution of simulated  $P_S$  values.

## Acknowledgments

We thank N. Barton, T. Cooper, J. Cuesta, J. Krug, A. Kalirad, S. Manrubia, I. Nemenman, and D. Weissman, for helpful discussions. A. Kalirad and I. Patanam contributed to coding, testing, and documentation.

## Additional information

### Funding

| Funder   | Grant reference number | Author       |
|--|------------------------|--------------|
| European Research Council  | ERC-2009-AdG-250152    |              |
|  | SELECTIONINFORMATION   | TP           |
| Max Planck Institute for the<br>Physics of Complex Systems   |                        | KEB and RBRA |
| National Science Foundation  | DEB-1354952            | RBRA         |
| National Science Foundation  | DMR-1206839            | KEB          |
| National Science Foundation  | EF-0742803             | RBRA         |
| National Institutes of Health  | R01GM101352            | RBRA         |
| Portuguese Foundation for<br>Science and Technology  |                        | TP           |
| Wissenschaftskolleg zu Berlin  |                        | RBRA         |
| The funders had no role in study design, data collection and interpretation, or the decision to submit the work for publication. |                        |              |

### Competing interests

The authors declare no competing financial interests.

### Author contributions

The project was initiated by TP and RBRA. TP wrote preliminary code and collected preliminary data. This study was conceived, performed and interpreted primarily by RBRA, with contributions from both TP and KEB. The manuscript was written primarily by RBRA, with contributions from both TP and KEB.

## References

- Agrawal AF, Feder JL, Nosil P. 2011. Ecological divergence and the origins of intrinsic postmating isolation with gene flow. *Int J Ecol* **2011**:435357. doi:10.1155/2011/435357.
- Ancel LW, Fontana W. 2000. Plasticity, evolvability, and modularity in RNA. *J Exp Zool (Mol Dev Evol)* **288**:242–283. doi:10.1002/1097-010X(20001015)288:3<242::AID-JEZ5>3.0.CO;2-O.
- Bank C, Bürger R, Hermisson J. 2012. The limits to parapatric speciation: Dobzhansky–Muller incompatibilities in a continent–island model. *Genetics* **191**:845–863. doi:10.1534/genetics.111.137513.
- Barton NH. 1996. Natural selection and random genetic drift as causes of evolution on islands. *Phil Trans R Soc B* **351**:785–795. doi:10.1098/rstb.1996.0073.

- Barton NH, Bengtsson BO. 1986. The barrier to genetic exchange between hybridising populations. *Heredity* **56**:357–376. doi:10.1038/hdy.1986.135.
- Barton NH, de Cara MAR. 2009. The evolution of strong reproductive isolation. *Evolution* **63**:1171–1190. doi:10.1111/j.1558-5646.2009.00622.x.
- Bengtsson BO, Christiansen FB. 1983. A two-locus mutation-selection model and some of its evolutionary implications. *Theor Popul Biol* **24**:59–77. doi:10.1016/0040-5809(83)90046-1.
- Bergman A, Feldman MW. 1992. Recombination dynamics and the fitness landscape. *Physica D* **56**:57–67. doi:10.1016/0167-2789(92)90050-W.
- Boerlijst MC, Bonhoeffer S, Nowak MA. 1996. Viral quasi-species and recombination. *Proc R Soc B* **263**:1577–84. doi:10.1098/rspb.1996.0231.
- Bürger R. 1989. Linkage and the maintenance of heritable variation by mutation-selection balance. *Genetics* **121**:175–184.
- Cabot EL, Davis AW, Johnson NA, Wu CI. 1994. Genetics of reproductive isolation in the *Drosophila simulans* clade: complex epistasis underlying hybrid male sterility. *Genetics* **137**:175–189.
- Carson HL, Templeton AR. 1984. Genetic revolutions in relation to speciation phenomena: the founding of new populations. *Annu Rev Ecol Syst* **15**:97–131. doi:10.1146/annurev.es.15.110184.000525.
- Corbett-Detig RB, Zhou J, Clark AG, Hartl DL, Ayroles JF. 2013. Genetic incompatibilities are widespread within species. *Nature* **504**:135–7. doi:10.1038/nature12678.
- Csárdi G, Nepusz T. 2006. The igraph software package for complex network research. *InterJournal Complex Systems* **1695**.
- Cutter AD. 2012. The polymorphic prelude to Bateson–Dobzhansky–Muller incompatibilities. *Tr Ecol Evol* **27**:209–218. doi:10.1016/j.tree.2011.11.004.
- Dobzhansky T. 1937. *Genetics and the origin of species*. New York: Columbia Univ. Press.
- Draghi JA, Parsons TL, Wagner GP, Plotkin JB. 2010. Mutational robustness can facilitate adaptation. *Nature* **463**:353–355. doi:10.1038/nature08694.
- Estrada E, Rodríguez-Velázquez JA. 2005. Subgraph centrality in complex networks. *Phys Rev E* **71**:056103. doi:10.1103/PhysRevE.71.056103.
- Faria R, Navarro A. 2010. Chromosomal speciation revisited: rearranging theory with pieces of evidence. *Tr Ecol Evol* **25**:660–669. doi:10.1016/j.tree.2010.07.008.
- Felsenstein J. 1981. Skepticism towards Santa Rosalia, or why are there so few kinds of animals? *Evolution* **35**:124–138. doi:10.2307/2407946.

- Flaxman SM, Wacholder AC, Feder JL, Nosil P. 2014. Theoretical models of the influence of genomic architecture on the dynamics of speciation. *Mol Ecol* **23**:4074–4088. doi:10.1111/mec.12750.
- Force A, Lynch M, Pickett FB, Amores A, Yan YL, Postlethwait J. 1999. Preservation of duplicate genes by complementary, degenerative mutations. *Genetics* **151**:1531–1545.
- Fraïsse C, Elderfield JAD, Welch JJ. 2014. The genetics of speciation: are complex incompatibilities easier to evolve? *J Evol Biol* **27**:688–699. doi:10.1111/jeb.12339.
- Gavrilets S. 1997. Hybrid zones with Dobzhansky-type epistatic selection. *Evolution* **51**:1027–1035. doi:10.2307/2411031.
- Gavrilets S. 1999. A dynamical theory of speciation on holey adaptive landscapes. *Am Nat* **154**:1–22. doi:10.1086/303217.
- Gavrilets S. 2004. *Fitness landscapes and the origin of species*. Princeton, NJ: Princeton Univ. Press.
- Gavrilets S, Gravner J. 1997. Percolation on the fitness hypercube and the evolution of reproductive isolation. *J Theor Biol* **184**:51–64. doi:10.1006/jtbi.1996.0242.
- Gavrilets S, Hastings A. 1996. Founder effect speciation: A theoretical reassessment. *Am Nat* **147**:466–491. doi:10.2307/2463218.
- Gavrilets S, Li H, Vose MD. 1998. Rapid parapatric speciation on holey adaptive landscapes. *Proc R Soc B* **265**:1483–9. doi:10.1098/rspb.1998.0461.
- Hagberg AA, Schult DA, Swart PJ. 2008. Exploring network structure, dynamics, and function using NetworkX. In: *Proceedings of the 7th Python in Science Conference (SciPy2008)*. Pasadena, CA, pp. 11–15.
- Higgs PG. 1998. Compensatory neutral mutations and the evolution of RNA. *Genetica* **102-103**:91–101. doi:10.1023/A:1017059530664.
- Huynen MA, Stadler PF, Fontana W. 1996. Smoothness within ruggedness: the role of neutrality in adaptation. *Proc Natl Acad Sci U S A* **93**:397–401. doi:10.1073/pnas.93.1.397.
- Jacobi MN, Nordahl M. 2006. Quasispecies and recombination. *Theor Popul Biol* **70**:479–485. doi:10.1016/j.tpb.2006.08.002.
- Jiménez JI, Xulvi-Brunet R, Campbell GW, Turk-MacLeod R, Chen IA. 2013. Comprehensive experimental fitness landscape and evolutionary network for small rna. *Proc Natl Acad Sci U S A* **110**:14984–9. doi:10.1073/pnas.1307604110.
- Kimura M. 1952. “Stepping-stone” model of population. *Natl Inst Genet Japan* **3**:62–63.

- Kondrashov AS, Sunyaev S, Kondrashov FA. 2002. Dobzhansky–Muller incompatibilities in protein evolution. *Proc Natl Acad Sci U S A* **99**:14878–83. doi:10.1073/pnas.232565499.
- Kulathinal RJ, Bettencourt BR, Hartl DL. 2004. Compensated deleterious mutations in insect genomes. *Science* **306**:1553–1554. doi:10.1126/science.1100522.
- Lee Y, DSouza LM, Fox GE. 1997. Equally parsimonious pathways through an RNA sequence space are not equally likely. *J Mol Evol* **45**:278–284. doi:10.1007/PL00006231.
- Liou LW, Price TD. 1994. Speciation by reinforcement of premating isolation. *Evolution* **48**:1451–1459. doi:10.2307/2410239.
- Lipman DJ, Wilbur WJ. 1991. Modelling neutral and selective evolution of protein folding. *Proc R Soc B* **245**:7–11. doi:10.1098/rspb.1991.0081.
- Lynch M, Conery JS. 2000. The evolutionary fate and consequences of duplicate genes. *Science* **290**:1151–5.
- Lynch M, Force A. 2000a. The probability of duplicate gene preservation by subfunctionalization. *Genetics* **154**:459–473.
- Lynch M, Force AG. 2000b. The origin of interspecific genomic incompatibility via gene duplication. *Am Nat* **156**:590–605. doi:10.1086/316992.
- Maheshwari S, Barbash DA. 2011. The genetics of hybrid incompatibilities. *Annu Rev Genet* **45**:331–355. doi:10.1146/annurev-genet-110410-132514.
- Masly JP, Presgraves DC. 2007. High-resolution genome-wide dissection of the two rules of speciation in *Drosophila*. *PLoS Biol* **5**:e243. doi:10.1371/journal.pbio.0050243.
- Matute DR, Butler IA, Turissini DA, Coyne JA. 2010. A test of the snowball theory for the rate of evolution of hybrid incompatibilities. *Science* **329**:1518–1521. doi:10.1126/science.1193440. PMID: 20847270.
- Moyle LC, Nakazato T. 2010. Hybrid incompatibility “Snowballs” between solanum species. *Science* **329**:1521–1523. doi:10.1126/science.1193063. PMID: 20847271.
- Muller HJ. 1942. Isolating mechanisms, evolution and temperature. *Biol Symp* **6**:71–125.
- Nei M. 1976. Mathematical models of speciation and genetic distance. In: Karlin S, Nevo E, editors, *Population Genetics and Ecology*, New York: Academic Press, pp. 723–765.
- Nei M, Nozawa M. 2011. Roles of mutation and selection in speciation: From Hugo de Vries to the modern genomic era. *Genome Biol Evol* **3**:812–829. doi:10.1093/gbe/evr028.
- Newman MEJ. 2006. Modularity and community structure in networks. *Proc Natl Acad Sci U S A* **103**:8577–8582. doi:10.1073/pnas.0601602103.

- Newman MEJ. 2010. *Networks: an introduction*. Oxford: Oxford University Press.
- Oliphant TE. 2007. Python for scientific computing. *Comput Sci Eng* **9**:10–20. doi:10.1109/MCSE.2007.58.
- Orr HA. 1995. The population genetics of speciation: the evolution of hybrid incompatibilities. *Genetics* **139**:1805–1813.
- Orr HA, Turelli M. 2001. The evolution of postzygotic isolation: accumulating Dobzhansky-Muller incompatibilities. *Evolution* **55**:1085–1094. doi:10.1111/j.0014-3820.2001.tb00628.x.
- Otto SP. 2003. The advantages of segregation and the evolution of sex. *Genetics* **164**:1099–1118.
- Paixão T, Azevedo RBR. 2010. Redundancy and the evolution of *cis*-regulatory element multiplicity. *PLoS Comput Biol* **6**:e1000848. doi:10.1371/journal.pcbi.1000848.
- Paixão T, Bassler KE, Azevedo RBR. 2014. Data from: Emergent speciation by multiple dobzhansky–muller incompatibilities. *Dryad Digital Repository* doi:10.5061/dryad.8rr2g.
- Palmer ME, Feldman MW. 2009. Dynamics of hybrid incompatibility in gene networks in a constant environment. *Evolution* **63**:418–431. doi:10.1111/j.1558-5646.2008.00577.x.
- Park SC, Krug J. 2011. Bistability in two-locus models with selection, mutation, and recombination. *J Math Biol* **62**:763–788. doi:10.1007/s00285-010-0352-x.
- Payseur BA, Hoekstra HE. 2005. Signatures of reproductive isolation in patterns of single nucleotide diversity across inbred strains of mice. *Genetics* **171**:1905–1916. doi:10.1534/genetics.105.046193.
- Presgraves DC. 2003. A fine-scale genetic analysis of hybrid incompatibilities in *Drosophila*. *Genetics* **163**:955–972.
- Presgraves DC. 2010a. Darwin and the origin of interspecific genetic incompatibilities. *Am Nat* **176**:S45–S60. doi:10.1086/657058.
- Presgraves DC. 2010b. The molecular evolutionary basis of species formation. *Nat Rev Genet* **11**:175–180. doi:10.1038/nrg2718.
- Scannell DR, Byrne KP, Gordon JL, Wong S, Wolfe KH. 2006. Multiple rounds of speciation associated with reciprocal gene loss in polyploid yeasts. *Nature* **440**:341–345. doi:10.1038/nature04562.
- Schluter D. 2009. Evidence for ecological speciation and its alternative. *Science* **323**:737–741. doi:10.1126/science.1160006.
- Schumer M, Cui R, Powell DL, Dresner R, Rosenthal GG, Andolfatto P. 2014. High-resolution mapping reveals hundreds of genetic incompatibilities in hybridizing fish species. *eLife* **3**:e02535. doi:10.7554/eLife.02535.

- Schuster P, Fontana W, Stadler PF, Hofacker IL. 1994. From sequences to shapes and back: a case study in RNA secondary structures. *Proc R Soc B* **255**:279–284. doi:10.1098/rspb.1994.0040.
- Seehausen O, Butlin RK, Keller I, Wagner CE, Boughman JW, Hohenlohe PA, Peichel CL, Saetre GP, Bank C, Brännström A, Brelsford A, Clarkson CS, Eroukhmanoff F, Feder JL, Fischer MC, Foote AD, Franchini P, Jiggins CD, Jones FC, Lindholm AK, Lucek K, Maan ME, Marques DA, Martin SH, Matthews B, Meier JI, Möst M, Nachman MW, Nonaka E, Rennison DJ, Schwarzer J, Watson ET, Westram AM, Widmer A. 2014. Genomics and the origin of species. *Nat Rev Genet* **15**:176–92. doi:10.1038/nrg3644.
- Servedio MR, Kirkpatrick M. 1997. The effects of gene flow on reinforcement. *Evolution* **51**:1764–1772. doi:10.2307/2410999.
- Szöllősi GJ, Derényi I. 2008. The effect of recombination on the neutral evolution of genetic robustness. *Math Biosci* **214**:58–62. doi:10.1016/j.mbs.2008.03.010.
- Templeton AR. 1980. The theory of speciation via the founder principle. *Genetics* **94**:1011–1038.
- van Nimwegen E, Crutchfield JP, Huynen M. 1999. Neutral evolution of mutational robustness. *Proc Natl Acad Sci U S A* **96**:9716–9720. doi:10.1073/pnas.96.17.9716.
- Wagner A. 2008. Robustness and evolvability: a paradox resolved. *Proc R Soc B* **275**:91–100. doi:10.1098/rspb.2007.1137.
- Wagner A. 2011. The low cost of recombination in creating novel phenotypes. *BioEssays* **33**:636–646. doi:10.1002/bies.201100027.
- Wagner A, Wagner GP, Simillion P. 1994. Epistasis can facilitate the evolution of reproductive isolation by peak shifts: a two-locus two-allele model. *Genetics* **138**:533–545.
- Weinreich DM, Lan Y, Wylie CS, Heckendorn RB. 2013. Should evolutionary geneticists worry about higher-order epistasis? *Curr Opin Genet Dev* **23**:700–707. doi:10.1016/j.gde.2013.10.007.
- Welch JJ. 2004. Accumulating Dobzhansky-Muller incompatibilities: Reconciling theory and data. *Evolution* **58**:1145–1156. doi:10.2307/3449212.
- Werth CR, Windham MD. 1991. A model for divergent, allopatric speciation of polyploid pteridophytes resulting from silencing of duplicate-gene expression. *Am Nat* **137**:515–526. doi:10.1086/285180.
- Wright AH, Rowe JE, Stephens CR, Poli R. 2003. Bistability in a gene pool GA with mutation. In: De Jong KA, Poli R, editors, *Foundations of Genetic Algorithms 7*, San Francisco: Morgan Kaufmann, pp. 63–80.
- Xia Y, Levitt M. 2002. Roles of mutation and recombination in the evolution of protein thermodynamics. *Proc Natl Acad Sci U S A* **99**:10382–10387. doi:10.1073/pnas.162097799.

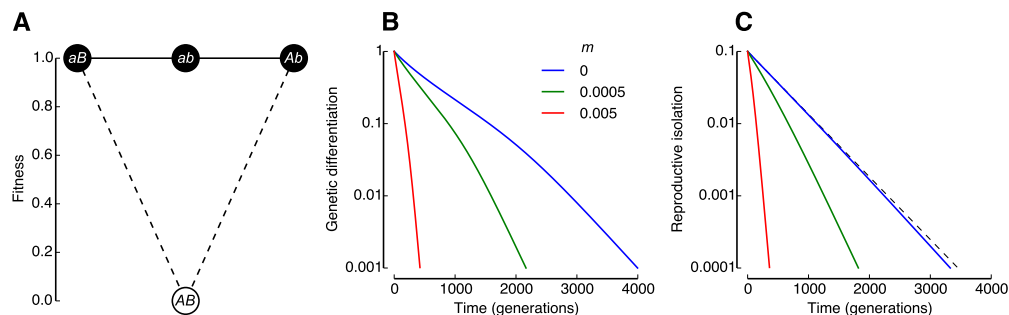


**Figure 1.** A neutral DMI between two loci is not sufficient to cause speciation. **(A)** Three haploid genotypes (closed circles) are fit and have equal fitness, and one genotype is unfit (open circle). The  $K = 3$  fit genotypes form a neutral network. **(B–C)** The reproductive isolation generated by a neutral DMI between two diallelic loci does not persist in the face of either mutation or gene flow because there is only one stable equilibrium (Figure 1—figure supplement 1). Two populations start fixed for the *Ab* and *aB* genotypes, respectively, and are allowed to evolve with a mutation rate of  $u = 10^{-3}$  per locus per generation, a recombination rate of  $r = 0.2$  between loci, and in the presence of different levels of gene flow ( $m$ , proportion of a the population consisting of migrants from the other population, each generation). Genotypes are only allowed to mutate at one locus per generation. **(B)** Genetic differentiation ( $G_{ST}$ ) and **(C)** degree of reproductive isolation ( $I$ ) between the two populations (see Materials and methods). Initially,  $G_{ST} = 1$  and  $I_0 = r/2 = 0.1$ . The dashed line in **(C)** shows  $I_t = I_0 \cdot e^{-2ut}$ . For raw data, see data/fig\_1/; for code, see ipython/fig\_1.ipynb (Dryad: Paixão et al., 2014).

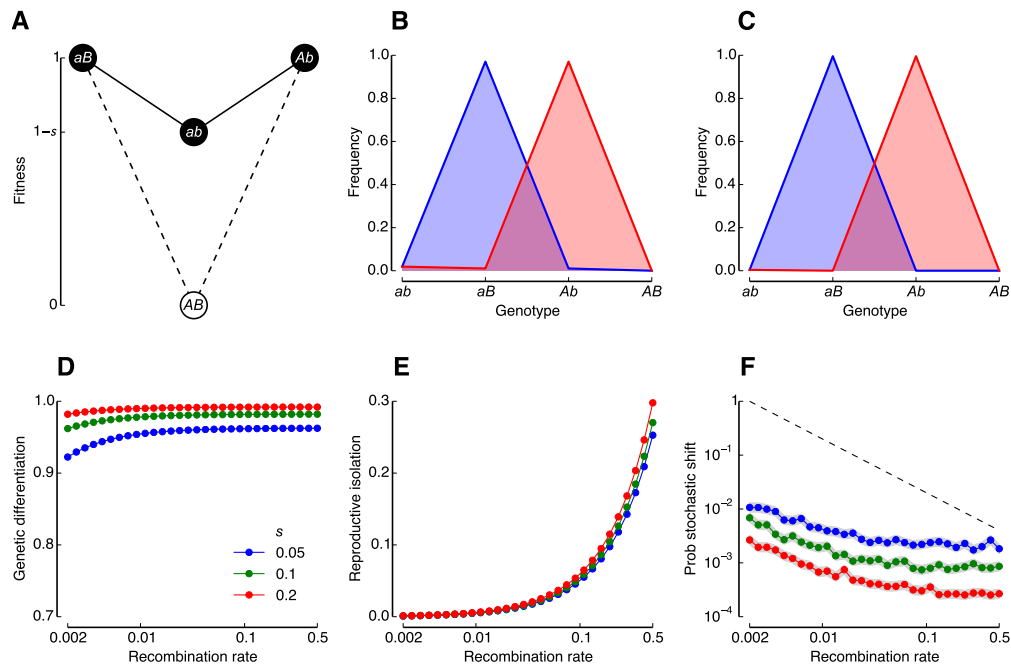


**Figure 2.** Selection for derived alleles in a single DMI increases the number of stable equilibria. (A) Fitness landscape generated by a single DMI between  $L = 2$  diallelic loci with selection for derived alleles.  $s$  measures the strength of selection against the  $ab$  genotype. This is an example of a “mutation-order” model (Schluter, 2009) because it assumes that the different populations experience the same environment. Note that if  $s = 1$ , the  $ab$  genotype is lethal and the model reduces to a disconnected neutral network with two genotypes:  $aB$  and  $Ab$ . (B–C) If both  $r$  and  $s \gg u$ , then there are two stable equilibria, one with  $\hat{p}_{Ab} \approx 1$  and the other with  $\hat{p}_{aB} \approx 1$ . (B) Weak recombination and selection ( $r = 0.002$ ,  $s = 0.05$ ). (C) Strong recombination and selection ( $r = 0.5$ ,  $s = 0.2$ ). Both the genetic differentiation (D) and the reproductive isolation (E) among populations at the two stable equilibria increases with both  $s$  and  $r$ . The degree of reproductive isolation is well approximated by  $I \approx r(1 + s)/2$ . (F) The probability that a founder event causes a stochastic shift ( $P_S$ ) from one stable equilibrium to the other decreases with both  $s$  and  $r$ . A new population was founded by taking a sample of  $N_0 = 2$  individuals from a population at the blue equilibrium, and was allowed to double in size every generation ( $\lambda = 2$ , see Materials and methods).  $P_S$  was calculated based on 100 successful shifts to the red equilibrium. The shaded area shows the 95% confidence interval of each data point. The dashed line shows  $0.002/r$ . Population genetic parameters:  $u = 10^{-3}$  per locus; genotypes are allowed to mutate at both loci per generation. For raw data, see data/fig\_2/; for code, see ipython/fig\_2.ipynb (Dryad: Paixão et al., 2014).

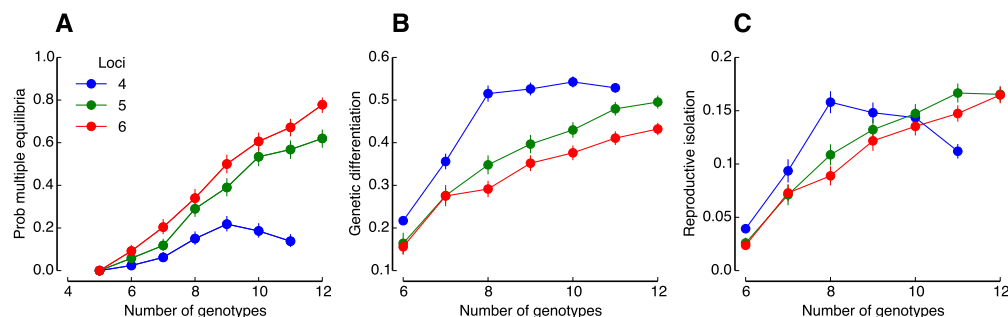


**Figure 3.** Larger neutral networks are more likely to contain multiple stable equilibria. **(A)** Probability that random neutral networks containing  $K$  genotypes of  $L$  diallelic loci contain multiple stable equilibria ( $P_M$ ). Values are estimates based on ensembles of 500 random connected neutral networks for each combination of  $K$  and  $L$ . None of the neutral networks could have been specified by a single DMI of any order ( $2 \leq \omega \leq L$ ). Genetic differentiation **(B)** and degree of reproductive isolation **(C)** between populations at different equilibria. In **(B–C)** values are means for neutral networks containing two or more stable equilibria (if a neutral network contained more than two stable equilibria, the maximum pairwise  $G_{ST}$  and  $I$  were used). All error bars are 95% confidence intervals. Population genetic parameters:  $r = \frac{1}{2(L-1)}$  between adjacent loci; up to  $L - 1$  crossovers are allowed between two genotypes per generation;  $u = r/20$  per locus per generation; genotypes are only allowed to mutate at  $L - 2$  loci per generation.  $P_M$  is affected by the number of alleles per locus ( $\alpha$ ) (Figure 3—figure supplement 1), by network properties of the neutral networks (Table 1; Figure 3—figure supplement 2; Figure 3—figure supplement 3) and by the pattern of recombination between sites (Figure 3—figure supplement 4). For raw data, see data/fig.3/; for code, see ipython/fig.3.ipynb (Dryad: Paixão et al., 2014).

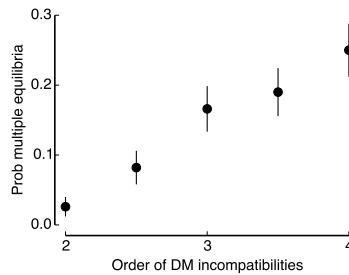


**Figure 4.** Higher-order incompatibilities increase the probability that the resulting neutral network shows multiple stable equilibria. Values are probabilities that neutral networks show multiple stable equilibria ( $P_M$ ). Each estimate is based on an ensemble of 500 random connected neutral networks of  $K = 9$  genotypes generated from random combinations of DMIs of a given order ( $\omega$ ) between alleles at  $L = 6$  diallelic loci. Integer values of  $\omega$  indicate that the neutral networks are specified entirely by  $d$  DMIs of order  $\omega$ . Values of  $\omega$  of the form  $\phi + 1/2$  indicate that the neutral networks are specified by  $d/2$  DMIs of order  $\phi$  and  $d/2$  DMIs of order  $\phi + 1$  ( $d$  even). The value of  $d$  in each neutral network in an ensemble was drawn at random from a broad uniform distribution. Then  $d$  DMIs with certain  $\omega$  were sampled without replacement. A neutral network was then generated from these DMIs and retained for further analysis if it had  $K = 9$ . Error bars are 95% confidence intervals. Population genetic parameters:  $r = \frac{1}{2(L-1)}$  between adjacent loci; up to  $L - 1$  crossovers are allowed between two genotypes per generation;  $u = r/20$  per locus per generation; genotypes are only allowed to mutate at two loci per generation. For raw data, see data/fig\_4/; for code, see ipython/fig\_4.ipynb (Dryad: Paixão et al., 2014).

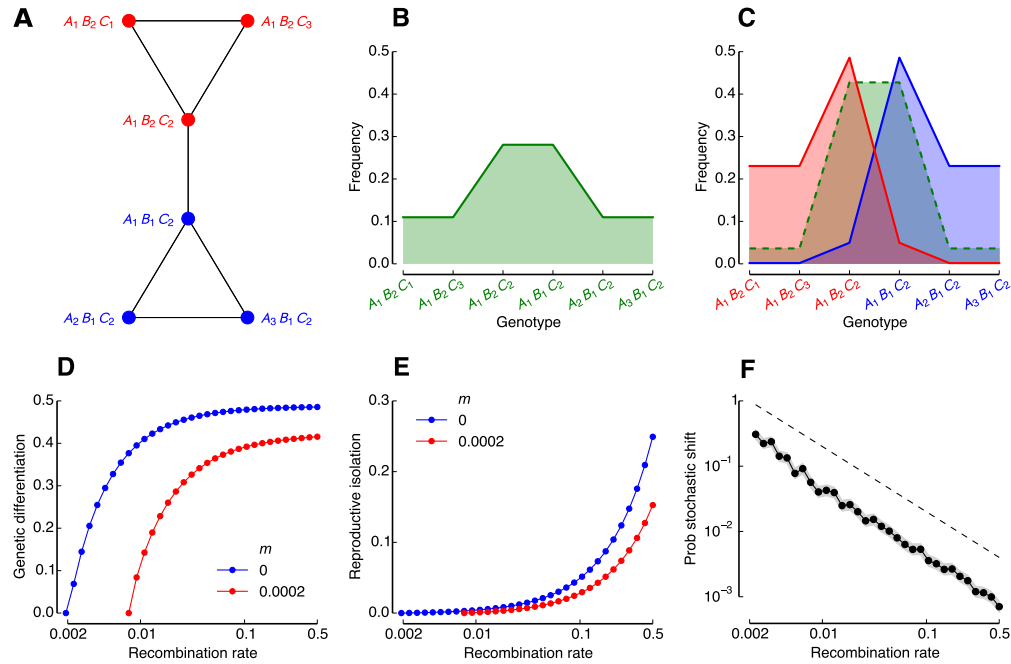


**Figure 5.** Increasing the recombination rate between DMI loci promotes emergent speciation. **(A)** Neutral network of  $K = 6$  genotypes including all genotypes containing either the  $A_1 B_2$  haplotype (red) or the  $B_1 C_2$  haplotype (blue). Genotypes are represented by closed circles. Solid lines connect genotypes differing at a single locus. The colors relate to the equilibria as explained below. **(B–C)** The presence of multiple stable equilibria in the neutral network shown in **(A)** depends on the recombination rate ( $r$ ). Populations initially fixed for a genotype shown in a given color, evolve to a stable equilibrium shown in the same color. **(B)** When the recombination rate is low ( $r = 10^{-3}$ ), populations initially fixed for any of the genotypes in the neutral network evolve to the same stable equilibrium. **(C)** With higher recombination rate ( $r = 10^{-2}$ ), populations initially fixed for any of 3 genotypes shown in red evolve to the stable equilibrium in red, whereas populations initially fixed one of the 3 genotypes shown in blue evolve to the stable equilibrium in blue. Populations showing perfectly even genotype frequencies evolve to the unstable equilibrium in green. The critical value of  $r$  at which the equilibria bifurcate depends on  $u$  (Figure 5—figure supplement 1). Both the genetic differentiation **(D)** and the reproductive isolation **(E)** among populations at the two stable equilibria increase with  $r$ , and can persist in the presence of weak gene flow (see also, Figure 5—figure supplement 2), changes in the fitness of genotypes in the neutral network (Figure 5—figure supplement 3), and increases in the fitness of genotypes outside the neutral network (Figure 5—figure supplement 4). The blue points are well approximated by  $I = r/2$ , the maximum reproductive isolation attainable with one neutral DMI (Figure 1). **(F)** Probability that a founder event causes a stochastic shift ( $P_S$ ) from one stable equilibrium to the other decreases with  $r$ . A new population was founded by taking a sample of  $N_0 = 2$  individuals from a population at the blue equilibrium, and was allowed to double in size every generation ( $\lambda = 2$ , see Materials and methods).  $P_S$  was calculated based on 100 successful shifts to a red equilibrium. The shaded area shows the 95% confidence interval of each data point. The dashed line shows  $0.002/r$ . Population genetic parameters:  $u = 10^{-3}$  per locus; genotypes are allowed to mutate at all loci per generation; up to two crossovers were allowed between two genotypes. For raw data, see data/fig\_5/; for code, see ipython/fig\_5.ipynb (Dryad: Paixão et al., 2014).

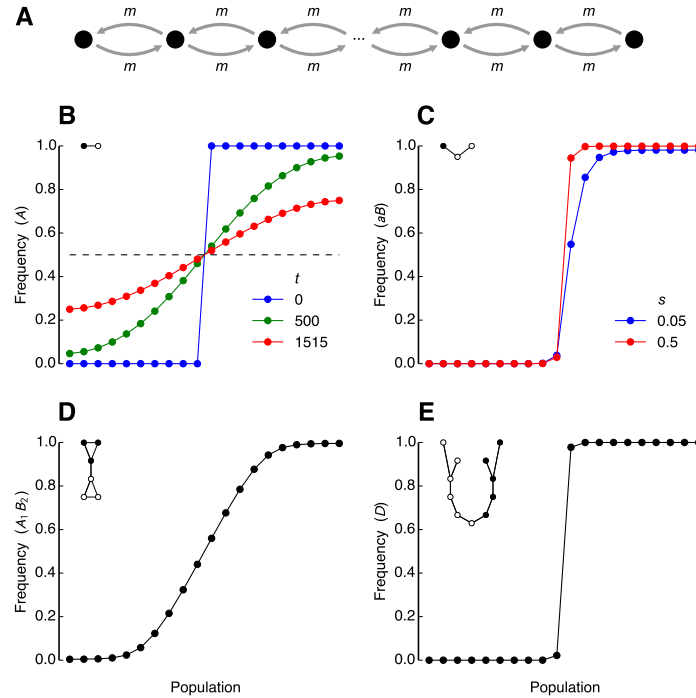


**Figure 6.** Neutral DMIs can generate strong reproductive barriers. **(A)** Stepping-stone model. A number  $n$  of populations are arranged in a line. Every generation a proportion  $2m$  of a population emigrates to its two neighboring populations (except populations 1 and  $n$ , which have only one neighbor, so only  $m$  of each of them emigrate) (see Materials and methods for more details). **(B)** Spread of a neutral allele over  $n = 20$  populations. Locus A has two neutral alleles,  $A$  and  $a$ . Initially, populations 1–10 are fixed for the  $a$  allele and populations 11–20 are fixed for the  $A$  allele (blue). We allow the populations to evolve with  $m = 0.025$ , without mutation at the A locus. The green points show the frequencies of the  $A$  allele after  $t = 500$  generations. After  $t = 1515$  generations, the frequency of  $A$  has increased from 0 to 25% in population 1 ( $T_N$  in Table 2). Eventually, the population will reach equilibrium with each neutral allele at a frequency of 50% in every population (dashed line). **(C–E)** Equilibrium allele or genotype frequencies in a hybrid zone formed after the contact of two populations initially at different stable equilibria on opposite ends of the line. See Table 2 for analysis of flow of unlinked neutral alleles through these hybrid zones. **(C)** DMI with selection (Figure 2). Initially, populations 1–10 are fixed for the  $Ab$  genotype and populations 11–20 are fixed for the  $aB$  genotype. The points show the equilibrium frequencies of  $aB$  for  $r = 0.5$  and  $m = 0.025$  and different values of  $s$ . **(D)** Neutral network shown in Figure 5. Initially, populations 1–10 are fixed for the  $B_1C_2$  haplotype and populations 11–20 are fixed for the  $A_1B_2$  haplotype. The points show the equilibrium frequencies of the  $A_1B_2$  haplotype for  $r = 0.5$  and  $m = 0.025$ . **(E)** Neutral network shown in Figure 7. Initially, populations 1–10 are fixed for the  $d$  allele and populations 11–20 are fixed for the  $D$  allele (a rough marker for the red equilibrium in Figure 7). The points show the equilibrium frequencies of the  $D$  allele for  $r = 0.5$  and  $m = 0.025$ . Population genetic parameters in **(C–E)**:  $u = 10^{-3}$  per locus; genotypes are only allowed to mutate at one locus per generation; up to  $L - 1$  crossovers are allowed between two genotypes per generation. For raw data, see data/fig.2/, data/fig.5/ and data/fig.7/; for code, see ipython/fig.6.ipynb (Dryad: Paixão et al., 2014).

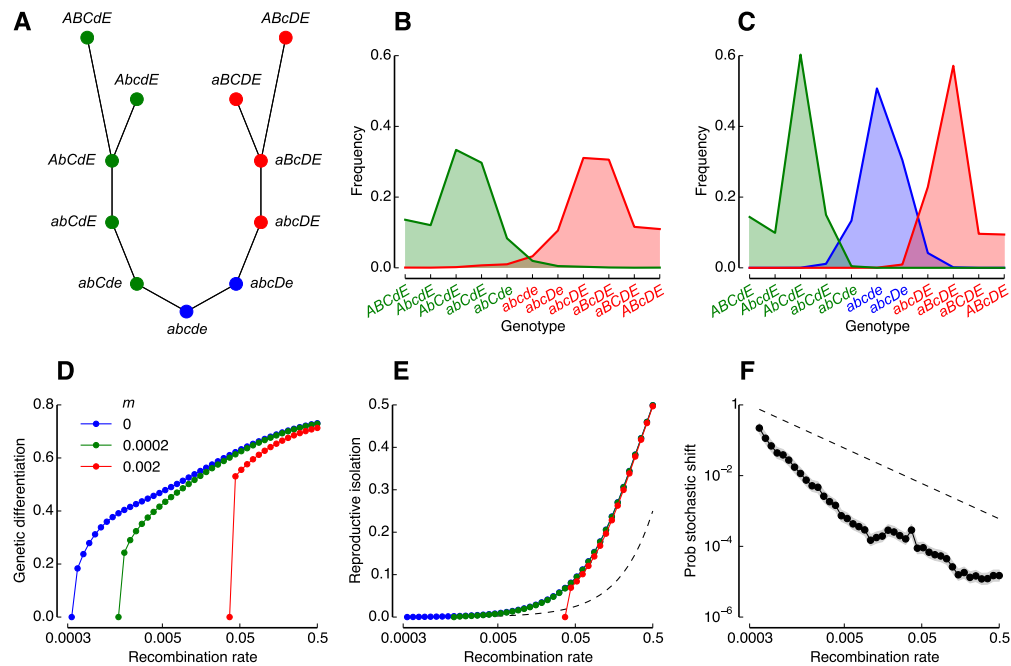


**Figure 7.** Multiple neutral DM incompatibilities can generate substantial reproductive barriers. (A) Neutral network of  $K = 11$  genotypes generated by 9 DMIs between  $L = 5$  diallelic loci. Genotypes are represented by closed circles. Solid lines connect genotypes differing at a single locus. The colors relate to the equilibria as explained below. (B–C) The presence of multiple stable equilibria in the neutral network shown in (A) depends on the recombination rate. When the recombination rate is low ( $0 \leq r \leq 3.6 \times 10^{-4}$ ), populations initially fixed for any of the 11 genotypes in the neutral network evolve to the same stable equilibrium; when the recombination rate is higher ( $3.6 \times 10^{-4} \leq r \leq 5.3 \times 10^{-3}$ ), there are two stable equilibria; when the recombination rate is higher still ( $5.3 \times 10^{-3} \leq r \leq 0.5$ ) there are three stable equilibria. (B) When  $r = 10^{-3}$ , populations initially fixed for any of 7 genotypes shown in red evolve to the stable equilibrium in red, whereas populations initially fixed one of the 5 genotypes shown in green evolve to the stable equilibrium in green. (C) When  $r = 10^{-2}$ , populations initially fixed for genotypes shown in red, green or blue (same colors in (A)), evolve to the equilibrium of the same color. Both the genetic differentiation (D) and the reproductive isolation (E) among populations at the red and green equilibria increases with the recombination rate, and can persist in the presence of substantial amounts of gene flow. The dashed line in (E) shows  $I = r/2$ , the maximum value of reproductive isolation attainable with one neutral DMI (Figure 1). The reproductive barrier among populations can persist in the presence of weak gene flow (see also, Figure 5—figure supplement 2), and changes in the fitness of genotypes in the neutral network (Figure 5—figure supplement 3). (F) Probability that a founder event causes a stochastic shift ( $P_S$ ) from one stable equilibrium to the other decreases with  $r$ . A new population was founded by taking a sample of  $N_0 = 2$  individuals from a population at the green equilibrium, and was allowed to double in size every generation ( $\lambda = 2$ , see Materials and methods).  $P_S$  was calculated based on 30 successful shifts to a red equilibrium. The shaded area shows the 95% confidence interval of each data point. The dashed line shows  $0.0003/r$ . Population genetic parameters:  $u = 10^{-3}$  per locus; genotypes are allowed to mutate at up to two loci per generation; up to four crossovers were allowed between two genotypes. For raw data, see data/fig\_7/; for code, see ipython/fig\_7.ipynb (Dryad: Paixão et al., 2014).

**Table 1.** The network properties of neutral networks influence the probability that they contain multiple stable equilibria.

| Network property             | $\rho(\text{SR})$ | $\rho(\text{DA})$ | $z$   |
|------------------------------|-------------------|-------------------|-------|
| Algebraic connectivity       | 0.926             | 0.074             | -6.79 |
| Average degree               | 0.851             | 0.118             | -8.23 |
| Average Hamming distance     | -0.731            | 0.064             | 5.84  |
| Average shortest path length | -0.947            | 0.035             | 6.76  |
| Degree assortativity (DA)    | 0.021             | 1.000             | -7.80 |
| Estrada index                | 0.993             | -0.022            | -8.29 |
| Modularity                   | -0.857            | -0.105            | 8.87  |
| Spectral radius (SR)         | 1.000             | 0.021             | -8.98 |
| Variance in degree           | 0.777             | -0.408            | -3.74 |

The data are for the ensemble of 500 random networks with  $K = 9$  genotypes of  $L = 6$  diallelic loci (see Figure 3A, for more details). All the network statistics listed are associated with the probability that a random neutral network contains multiple stable equilibria,  $P_M$  ( $P < 0.001$ ; Figure 3—figure supplement 2). We conducted a separate logistic regression of  $P_M$  against each network statistic. The  $z$  statistic is the regression coefficient divided by its standard error. Most network statistics are strongly correlated with each other (see also Figure 3—figure supplement 3).  $\rho(\text{SR})$  and  $\rho(\text{DA})$  list the Spearman’s rank correlation coefficient between the network statistic and the spectral radius (SR) and degree assortativity (DA), respectively. All correlations with  $|\rho| > 0.4$  are highly statistically significant ( $P < 10^{-10}$ ). For raw data, see `data/tab_1/`; for code, see `ipython/tab_1.ipynb` (Dryad: Paixão et al., 2014).

**Table 2.** Multiple neutral DMIs can generate strong barriers to gene flow.

| Scenario                                     | $T_{25}$ | $b$    |
|--|----------|--------|
| DMI with selection (Figure 2)                |          |        |
| $s = 0.05$                                   | 1,556    | 1.0271 |
| $s = 0.1$                                    | 1,583    | 1.0449 |
| $s = 0.25$                                   | 1,632    | 1.0772 |
| $s = 0.5$                                    | 1,690    | 1.1155 |
| $s = 0.75$                                   | 1,742    | 1.1498 |
| $s = 1$                                      | 1,790    | 1.1815 |
| Neutral network                              |          |        |
| $K = 6$ , $L = 3$ , $\alpha = 3$ (Figure 5)  | 1,516    | 1.0007 |
| $K = 11$ , $L = 5$ , $\alpha = 2$ (Figure 7) | 1,797    | 1.1861 |

For each evolutionary scenario, we simulated a stepping-stone model with  $n = 20$  populations and  $m = 0.025$  between adjacent populations (see Materials and methods and Figure 6A). The rate of spread of a neutral allele at an unlinked locus across a reproductive barrier created by a set of DMIs was used to evaluate the strength of the barrier. Populations 1–10 and 11–20 are initialized at different stable equilibria. The populations are then allowed to evolve with gene flow until they reach a new equilibrium (Figure 6C–E). Then populations 1–10 and 11–20 are fixed for different neutral alleles at a locus unlinked to any of the fitness loci, and allowed to continue evolving. The genotype frequencies for the fitness loci remain at equilibrium, but the frequencies of the neutral alleles begin to evolve towards 0.5 (Figure 6B).  $T_{25}$  measures the time required for the frequency of one of the neutral alleles to increase from 0 to 25% in population 1.  $b = T_{25}/T_N$  measures the strength of the barrier to gene flow where  $T_N = 1515$  is the  $T_{25}$  for a neutral allele at a single locus (Figure 6B). If  $b > 1$ , the reproductive barrier impedes the flow of a neutral allele. Population genetic parameters:  $u = 10^{-3}$  per fitness locus and  $u = 0$  for the neutral marker locus; genotypes are only allowed to mutate at one fitness locus per generation; there is free recombination ( $r = 0.5$ ) between all loci. For raw data, see [data/fig\\_2/](#), [data/fig\\_5/](#) and [data/fig\\_7/](#); for code, see [ipython/fig\\_7.ipynb](#) (Dryad: Paixão et al., 2014).

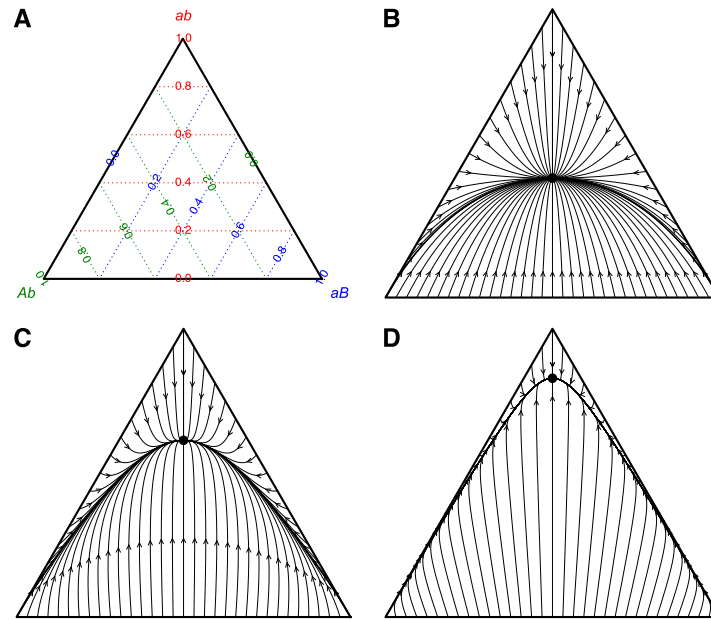


**Figure 1—figure supplement 1.** A neutral DMI between two diallelic loci (Figure 1A) only contains one stable equilibrium. **(A)** The frequencies of the three genotypes (*ab*, *Ab* and *aB*) in a population are represented as a single point in a ternary plot. **(B)** Evolutionary trajectories without recombination ( $r = 0$ ) of populations starting at initial frequencies such that at least one of the genotypes is absent (i.e., the edges of the triangle). All trajectories converge to a single stable equilibrium (solid circle) with frequencies  $\hat{p}_{Ab} = \hat{p}_{aB} = 1 - \frac{\sqrt{2}}{2}$  and  $\hat{p}_{ab} = \sqrt{2} - 1$ . Arrowheads mark the genotype frequencies after 100 generations of evolution. **(C–D)** Evolutionary trajectories with recombination rates of  $r = 0.01$  and  $0.1$ , respectively. As the recombination rate increases, the frequency of *ab* at equilibrium ( $\hat{p}_{ab}$ ) increases, and populations approach equilibrium more quickly. Population genetic parameters:  $u = 10^{-3}$  per locus per generation; genotypes are only allowed to mutate at one locus per generation. For code, see `ipython/fig_1_s1.ipynb` (Dryad: Paixão et al., 2014).

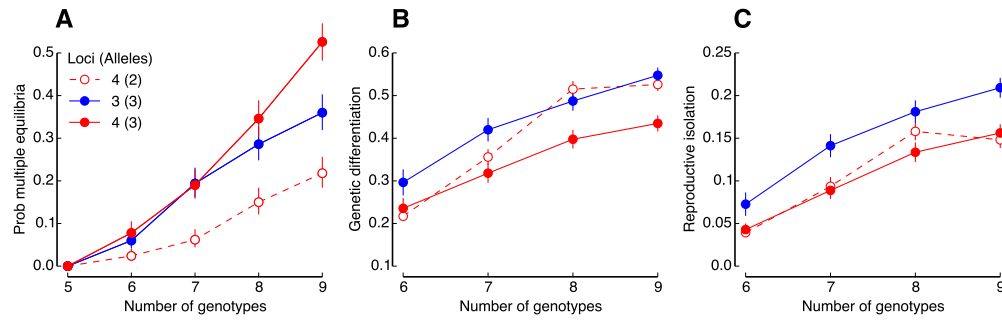


**Figure 3—figure supplement 1.** Larger neutral networks are more likely to contain multiple stable equilibria. **(A)** Probability that random neutral networks containing  $K$  genotypes of  $L$  loci with  $\alpha$  alleles contain multiple stable equilibria ( $P_M$ ). Expected genetic differentiation **(B)** and degree of reproductive isolation **(C)** between populations at different equilibria. The data for  $\alpha = 2$  alleles are the same as shown in Figure 3. See legend of Figure 3 for more details. For raw data, see data/fig\_3\_s1; for code, see ipython/fig\_3\_s1.ipynb (Dryad: Paixão et al., 2014).

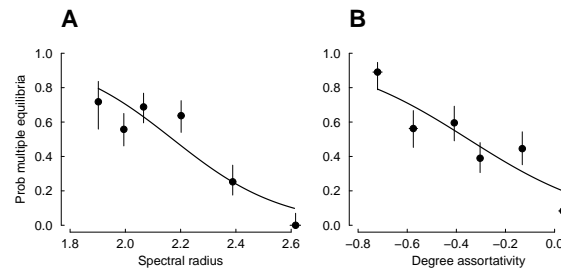


**Figure 3—figure supplement 2.** Network properties of neutral networks influence the probability that they contain multiple stable equilibria. To illustrate this, we show the relationship between two network properties and the probability that random neutral networks contain multiple stable equilibria ( $P_M$ ) (see Materials and methods for more details). **(A)**  $P_M$  is negatively related to the spectral radius of the adjacency matrix. The spectral radius is strongly correlated to several other network properties, including the algebraic connectivity, average degree, and modularity (Figure 3—figure supplement 3; Table 1). **(B)**  $P_M$  is negatively related to the degree assortativity. The degree assortativity is moderately correlated with the variance in degree of the neutral network (Table 1). The data are for the ensemble of 500 random networks with  $K = 9$  genotypes of  $L = 6$  diallelic loci that, overall, show  $P_M = 50\%$  (Figure 3A). Similar trends are observed for other values of  $K$ ,  $L$ , and  $\alpha$ . Values are probabilities and 95% confidence intervals for data grouped into approximately equal sized bins based on the network statistic. Solid lines show logistic regression fits to the raw data (see Table 1 for more details). For raw data, see data/tab\_1; for code, see ipython/fig\_3\_s2.ipynb (Dryad: Paixão et al., 2014).

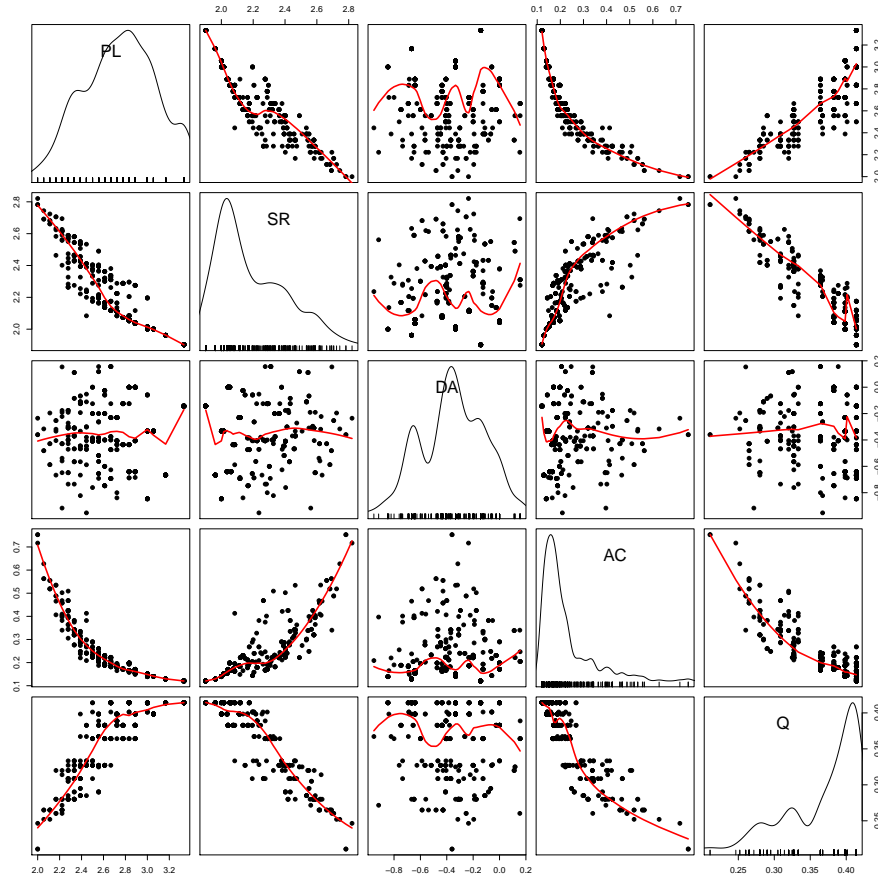


**Figure 3—figure supplement 3.** Network properties of neutral networks are correlated with each other. Network statistics (see Materials and methods): PL, average shortest path length; SR, spectral radius; DA, degree assortativity; AC, algebraic connectivity; Q, modularity. The data are the same as analysed in Table 1 and Figure 3—figure supplement 2. The diagonal shows kernel density and rug plots for each statistic. Red lines show locally weighted polynomial regression fits. All network statistics are strongly associated with  $P_M$ . For raw data, see data/tab.1; for code, see `ipython/fig_3_s3.ipynb` (Dryad: Paixão et al., 2014).

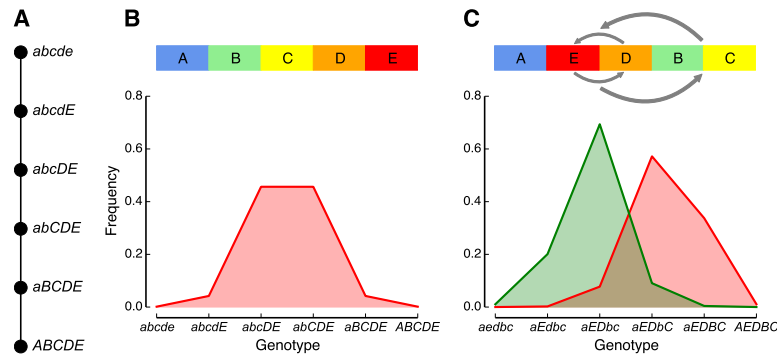


**Figure 3—figure supplement 4.** Whether or not a neutral network shows multiple stable equilibria depends on the precise pattern of recombination between sites and cannot be strictly predicted from the topology of the network. **(A)** Neutral network of  $K = 6$  genotypes generated by incompatibilities between  $L = 5$  loci. The shortest path length between two genotypes in the network is the same as the Hamming distance between them. **(B)** The neutral network shown in **(A)** shows a single stable equilibrium when the recombination rate is high relative to the mutation rate:  $r = \frac{1}{2(L-1)} = 0.125$  and  $u = r/20 = 0.00625$ . **(C)** The genotype network derived from that shown in **(A)** by inverting the D and E loci and inserting them between the A and B loci has the same topology and Hamming distances between genotypes as that in **(A)**, but shows two stable equilibria for the same values of  $r$  and  $u$  as in **(B)**. For raw data, see data/fig\_3.s4; for code, see ipython/fig\_3.s4.ipynb (Dryad: Paixão et al., 2014).

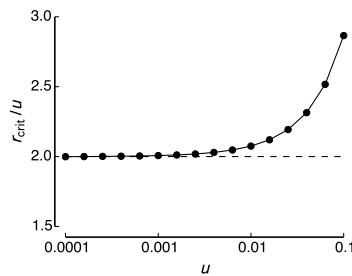


**Figure 5—figure supplement 1.** The critical point at which the equilibria bifurcate is approximately invariant with the ratio between the recombination rate ( $r$ ) and the mutation rate ( $u$ ). We calculated the critical recombination rate ( $r_{\text{crit}}$ ) for different values of  $u$  (spanning 3 orders of magnitude) for the neutral network shown in Figure 5A. We did this by finding the point where the symmetric equilibrium (in green in Figures 5B and 5C) changes from stable to unstable. Population genetic parameters: genotypes are allowed to mutate at all loci per generation; up to two crossovers were allowed between two genotypes. For code, see ipython/fig\_5.s1.ipynb (Dryad: Paixão et al., 2014).

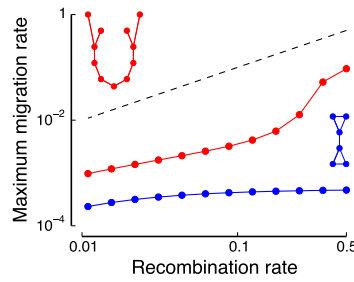


**Figure 5—figure supplement 2.** The reproductive barriers created by multiple neutral DMIs are robust to gene flow. Maximum migration rate between two populations that allows significant genetic differentiation between them to persist for different recombination rates. The analysis was carried out for the neutral networks shown in Figure 5A (blue) and Figure 7A (red). Population genetic parameters:  $u = 10^{-3}$  per locus; genotypes are allowed to mutate at up to two loci per generation; up to  $L-1$  crossovers were allowed between two genotypes. For raw data, see data/fig\_5/ and data/fig\_7/; for code, see `ipython/fig_5_s2.ipynb` (Dryad: Paixão et al., 2014).

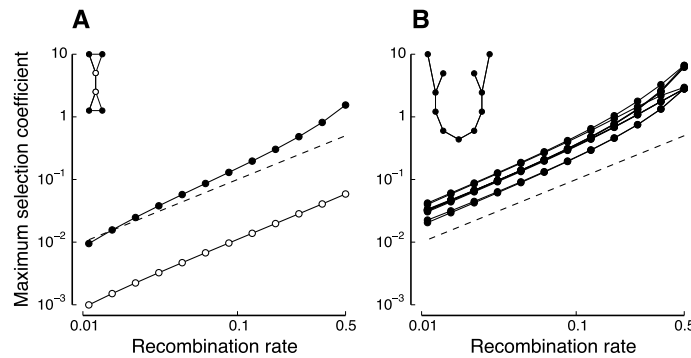


**Figure 5—figure supplement 3.** The reproductive barriers created by multiple neutral DMIs are robust to changes in the fitness of genotypes in the neutral network. The neutral network model assumes that “in-network” genotypes have a fitness of  $w = 1$ . Values show the maximum selection coefficient  $s_i$  by which the fitness of a genotype  $i$  in the neutral network can be increased ( $w_i = 1 + s_i$ ) while maintaining the existence of at least two stable equilibria. The analysis was carried out for the neutral networks shown in Figure 5A (A) and Figure 7A (B). The dashed lines show  $s = r$ . Population genetic parameters:  $u = 10^{-3}$  per locus; genotypes are allowed to mutate at up to two loci per generation; up to  $L-1$  crossovers were allowed between two genotypes. For raw data, see data/fig\_5/ and data/fig\_7/; for code, see `ipython/fig_5_s3.ipynb` (Dryad: Paixão et al., 2014).

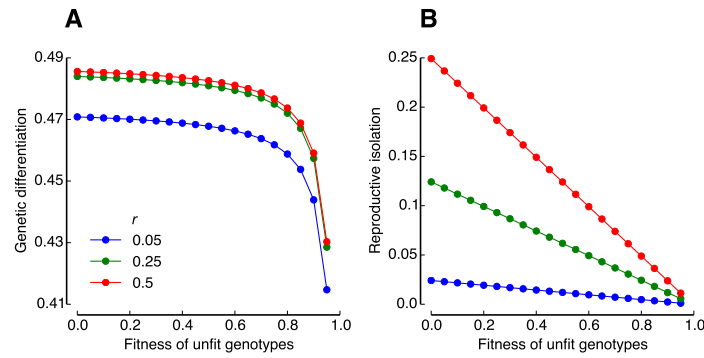


**Figure 5—figure supplement 4.** Partial DMIs can also cause emergent speciation. The neutral network model assumes that “out-of-network” genotypes have a fitness of  $w_{\text{out}} = 0$ . Here we measure the effect of changing  $w_{\text{out}}$  on the strength of the reproductive barriers evolving on the neutral network in Figure 5A. **(A)** The amount of genetic differentiation among populations at the two stable equilibria remains stable for  $w_{\text{out}} \lesssim 0.7$ . **(B)** The degree of reproductive isolation among populations at the two stable equilibria changes as  $I_0(1 - w_{\text{out}})$  where  $I_0$  is the reproductive isolation when  $w_{\text{out}} = 0$  (i.e., the default model). This is because higher values of  $w_{\text{out}}$  imply higher hybrid fitness. Population genetic parameters:  $u = 10^{-3}$  per locus; genotypes are allowed to mutate at all loci per generation; up to two crossovers were allowed between two genotypes. For code, see `ipython/fig_5_s4.ipynb` (Dryad: Paixão et al., 2014).